AMPK activation by SC4 inhibits noradrenaline-induced lipolysis and insulin-stimulated lipogenesis in white adipose tissue

Chuang, Sheng-Ju, Johanns, Manuel, dit Ruys, Sébastien, Steinberg, Gregory R., Kemp, Bruce Ernest E., Viollet, Benoit and Rider, Mark

Chuang, Sheng-Ju, Johanns, Manuel, dit Ruys, Sébastien, Steinberg, Gregory R., Kemp, Bruce Ernest E., Viollet, Benoit and Rider, Mark. (2022). AMPK activation by SC4 inhibits noradrenaline-induced lipolysis and insulin-stimulated lipogenesis in white adipose tissue. *Biochemical Journal,* 478(21), pp. 3869-3889. https://doi.org/10.1042/BCJ20210411

AMPK activation by SC4 inhibits noradrenaline-induced lipolysis and insulin-stimulated lipogenesis in white adipose tissue

by
Sheng-Ju Chuang[1], Manuel Johanns[1], Sébastien Pyr dit Ruys[1], Gregory R. Steinberg[2], Bruce E. Kemp[3,4], Benoît Viollet[5] and Mark H. Rider[1*]

[1]Université catholique de Louvain and de Duve Institute, Avenue Hippocrate 75, B-1200 Brussels, Belgium. [2]Centre for Metabolism, Obesity and Diabetes Research, Department of Medicine and Department of Biochemistry and Biomedical Sciences, McMaster University, Hamilton, Ontario, Canada. [3]St. Vincent's Institute of Medical Research and [3]Department of Medicine, University of Melbourne, Fitzroy, Victoria, Australia. [4]Mary MacKillop Institute for Health Research, Australian Catholic University, Fitzroy, VIC, Australia. [5]Université de Paris, Institut Cochin INSERM, CNRS, Paris, France.

Running title: AMPK activation inhibits adipose tissue insulin-stimulated lipogenesis

[*]Address for correspondence: Prof. Mark H. Rider, PHOS/SSS/DDUV, de Duve Institute-UCL, Avenue Hippocrate 75, bte B1.74.02, B-1200 Brussels, Belgium. Tel: + 32 2 764 7485; Fax: + 32 2 764 7507; E-mail: mark.rider@uclouvain.be

Synopsis
The effects of small-molecule AMP-activated protein kinase (AMPK) activators in rat epididymal adipocytes were compared. SC4 was the most effective and submaximal doses of SC4 and 5-amino-4-imidazolecarboxamide (AICA) riboside were combined to study effects of AMPK activation in white adipose tissue (WAT). Incubation of rat adipocytes with SC4 + AICA riboside inhibited noradrenaline-induced lipolysis and decreased hormone-sensitive lipase (HSL) Ser563 phosphorylation, without affecting HSL Ser565 phosphorylation. Preincubation of fat pads from wild-type (WT) mice with SC4 + AICA riboside inhibited insulin-stimulated lipogenesis from glucose or acetate and these effects were lost in AMPKα1 knockout (KO) mice, indicating AMPKα1 dependency. Moreover, in fat pads from acetyl-CoA carboxylase (ACC)1/2 S79A/S212A double knockin versus WT mice, the effect of SC4 + AICA riboside to inhibit insulin-stimulated lipogenesis from acetate was lost, pinpointing ACC as the main AMPK target. Treatment with SC4 + AICA riboside decreased insulin-stimulated glucose uptake, an effect that was still observed in fat pads from AMPKα1 KO versus WT mice, suggesting the effect was partly AMPKα1-independent. SC4 + AICA riboside treatment had no effect on the insulin-induced increase in palmitate esterification nor on *sn*-glycerol-3-phosphate-*O*-acyltransferase activity. Therefore in WAT, AMPK activation inhibits noradrenaline-induced lipolysis and suppresses insulin-stimulated lipogenesis primarily by inactivating ACC and by inhibiting glucose uptake.

Key words: AMPK; *de novo* lipogenesis; glucose transport; ACC; ACL; GPAT; TBC1D4

Abbreviations used: ACC, acetyl-CoA carboxylase; ACL, ATP-citrate lyase; AMPK, AMP-activated protein kinase; ATGL, adipose triglyceride lipase; GPAT, *sn*-glycerol-

3-phosphate-*O*-acyltransferase; HSL, hormone-sensitive lipase; PKB, protein kinase B; TBC1D4, Tre-2/BUB2/cdc 1 domain family 4.

Introduction

AMP-activated protein kinase (AMPK) is a highly conserved energy sensing eukaryotic protein kinase [1]. Once activated, AMPK switches on ATP-generating processes while simultaneously switching off energy consumption [1]. Canonical AMPK activation results from an increase in intracellular AMP:ATP ratio. Interestingly, physiological AMPK activation occurs in white adipose tissue (WAT) in response to stimulation by catecholamines [2] concomitant with an increase in AMP:ATP ratio as a result of the re-esterification of fatty acids released during lipolysis [3]. AMPK exists as heterotrimers comprising a catalytic α-subunit (α1 or α2) associated with regulatory β (β1 or β2) and γ (γ1, γ2 or γ3) subunits. In rat white adipocytes, AMPKα1-containing complexes have been reported to account for > 90 % of total AMPK activity [2] and AMPKβ1 is predominant, whereas mouse and human adipocytes express approximately equal levels of AMPKβ1 and AMPKβ2 [4].

The role of AMPK in metabolic control in liver and skeletal muscle has been studied extensively, but its roles in WAT are less well defined. Adult mice in which AMPK had been deleted in adipose tissue displayed increases in blood glucose and triglycerides [5], however the mechanisms mediating these effects are incompletely understood. AMPK activation has been proposed to be both pro- and anti-lipolytic or exert no effects [5,6]. AMPK activation was reported to be anti-lipolytic by phosphorylating hormone-sensitive lipase (HSL) [2,7,8]. However in human and rat adipocytes, AMPK activation by compound 991 (see below) did not inhibit the stimulation of lipolysis by isoproteranol [4]. On the other hand, AMPK was proposed to increase basal lipolysis via phosphorylation-induced activation of adipose triglyceride lipase (ATGL) [9]. Effects of AMPK activation on basal and insulin-stimulated glucose uptake in WAT are also ambiguous [6] and effects of AICA riboside and A-769662 (see below) to inhibit glucose uptake were recently reported to be AMPK-independent [10]. In addition to controlling lipolysis and glucose uptake, AMPK activation in WAT inhibits lipid synthesis by phosphorylating and inactivating acetyl-CoA carboxylase (ACC) [8], its best-known substrate, but could also have other sites of control in triglyceride (TG) synthesis. For example in liver, AMPK was proposed to cause phosphorylation-induced inactivation of mitochondrial *sn*-glycerol-3-phosphate-*O*-acyltransferase (GPAT) [11].

One of the reasons for potential discrepancies around the role of AMPK in adipose tissue involves the use of promiscuous pharmacological agents. AICA riboside was the first small-molecule pharmacological AMPK activator. AICA riboside enters cells and is converted to the AMP analogue ZMP, which then activates AMPK [12]. However, AICA riboside is non-specific due to the fact that ZMP can modulate the activities of other AMP-sensitive enzymes. A-769662 was the first direct AMPK activator [13-15] and is specific for AMPKβ1-containing complexes [16]. Compound 991 is also rather AMPKβ1-specific, at least in cell-free assays [17]. Both A-769662 and 991 allosterically increase AMPK activity and inhibit AMPKα Thr172 dephosphorylation. Other AMPKβ1-specific direct activators include PF-249, PF-06409577 and salicylate [18]. At high doses, 991 also activated AMPKβ2-containing complexes in skeletal muscle associated with increased glucose uptake [19]. A-769662 and 991 bind to a site located between the small lobe of the AMPK α-subunit kinase domain and the AMPK β-subunit CBM [17]. Since this site also binds

salicylate [20], the breakdown product of aspirin (acetyl salicylate), it has been called the "**A**llosteric **D**rug and **M**etabolite" or "ADaM" binding pocket [21]. Compounds SC4 [22], PF-739 [23] and MK-8722 [24] are "pan-β" direct AMPK activators that have recently been developed. Another small-molecule pan-AMPK activator is O304, the first to be used in human clinical trials [25], but its precise mode of action is unclear.

In the present study, we compared the efficacy of a panel of small-molecule AMPK activators in incubated rat adipocytes. SC4 was shown to be the most effective AMPK activator. A combination of submaximal doses of SC4 + AICA riboside was then used in incubated rat adipocytes to examine effects of AMPK activation on noradrenaline-induced lipolysis and in incubated mouse epididymal fat pads to investigate effects of AMPK activation on insulin-stimulated lipogenesis, glucose uptake and fatty acid esterification. AMPK activation by SC4 + AICA riboside was found to inhibit noradrenaline-induced lipolysis, possibly by decreasing HSL Ser563 phosphorylation. Also, SC4 + AICA riboside treatment reduced insulin-stimulated lipogenesis primarily by inactivating ACC and by inhibiting glucose uptake without affecting esterification.

Materials and methods

Materials

Insulin (Actrapid) was from Novo Nordisk. AICA riboside was from Sigma. All commercial antibodies were produced in rabbit or mouse whereas the anti-PDH antibodies were raised in sheep. Anti-total glyceraldehyde-3-phosphate dehydrogenase (GAPDH, MAB374; dilution 1:10000) antibody was from Merck-Millipore. Anti-total ACC (#3676; dilution 1:2000), anti-phospho Ser79 ACC (#11818; dilution 1:40000), anti-total AMPKα (#2532; dilution 1:2000), anti-phospho Thr172 AMPKα (#2535; dilution 1:2000), anti-total Raptor (#2280; dilution 1:2000), anti-phospho Ser792 Raptor (#2083; dilution 1:2000), anti-phospho Ser563 HSL (#4139; dilution 1:2000), anti-phospho Ser565 HSL (#4137; dilution 1:2000), anti-phospho HSL Ser660 ACL (#4126; dilution 1:2000), anti-total HSL (#4107; dilution 1:4000), anti-total ATGL (#2138; dilution 1:2000), anti-phospho Ser455 ATP-citrate lyase (ACL) (#4331; dilution 1:2000), anti-total Tre-2/BUB2/cdc 1 domain family 4 (TBC1D4, #2670; dilution 1:2000), anti-phospho Thr642 TBC1D4 (#8881; dilution 1:1000), anti-total protein kinase B (PKB)/Akt (#9272; dilution 1:2000), anti-phospho Thr308 PKB (#4056; dilution 1:2000) and anti-phospho Ser473 PKB (#4058; dilution 1:2000) antibodies were from Cell Signalling Technologies. Anti-total ACL (ab40793; dilution 1:1000) and anti-phospho Ser406 ATGL (ab135093; dilution 1:2000) antibodies were from Abcam. Anti-total pyruvate dehydrogenase (PDH) E1α (dilution 1:40000), anti-phospho Ser293 PDH E1α (dilution 1:40000) and anti-phospho Ser300 PDH E1α antibodies (dilution 1:40000) were kindly provided by Grahame Hardie (University of Dundee, UK). Compound 991 was kindly given by Kei Sakamoto (Nestlé, CH) and SC4 was kindly donated by Jonathan Oakhill (St. Vincent's Institute, University of Melbourne, AU). PF-739 and MK-8722 were purchased from Glixx Laboratories (Hopkinton, MA, USA). O304 (synthesized as HY112233 by MedChem Express) was from Bio-Connect (Te Huissen, Netherlands). [γ-^{32}P] ATP, [U-^{14}C] sodium acetate, [U-^{14}C] glucose, [9,10-^{3}H(N)] palmitate, [U-^{14}C] 2-deoxyglucose and [2-^{3}H] glycerol were purchased from Perkin Elmer. Palmitic acid was neutralized with NaOH at 65 °C and then bound to defatted albumin by adding the hot solution to a stirred solution of concentrated albumin which was then diluted in Krebs-Ringer Bicarbonate buffer (KRB) to give a stock solution of 2.5 mM palmitate in 5 % (w/v) albumin. "AMARA" peptide (for AMPK assay) was kindly

synthesized by Dr. V. Stroobant (Ludwig Institute, Brussels). Other chemicals were of standard or analytical grade obtained from MP Biomedicals, Thermo Fisher Scientific, Sigma-Aldrich, or Merck.

Animals

All animal experiments were approved by the Université catholique de Louvain Brussels local ethics committee (reference numbers 2017/UCL/MD/016 and 2021/UCL/MD/028) and conducted within the guidelines of the European Convention for the Protection of Vertebrate Animals used for Experimental and Other Scientific Purposes. Male Wistar rats (about 170 g of body weight) were obtained from the faculty animal house. ACC1/2 S79A/S212A double knockin (KI) mice [26], AMPKα1 knockout (KO) mice [27] and corresponding wild-type (WT) mice were maintained in the local animal house. All animals were maintained at a 12:12h light-dark cycle with free access to food and water and all animal experiments were carried out in the Protein Phosphorylation (PHOS) laboratory of the de Duve Institute, Université catholique de Louvain (UCLouvain), Brussels. Mice were anaesthetized by intraperitoneal injection of 20 mg/kg Rompun (xylazine) + 100 mg/kg Imalgene (ketamine). Rats were anaesthetized by intraperitoneal injection of 20 mg/kg Rompum (xylazine)+ 20 mg/kg Dolethal (sodium pentobarbital). After removal of adipose tissues, the animals were euthenised by cervical dislocation.

Incubation of freshly isolated rat epididymal adipocytes and mouse epididymal fat pads

Adipocytes were prepared from the epididymal fat pads of fed rats and incubated essentially as described [28]. Briefly, adipocytes were suspended in KRB containing 1 % (w/v) defatted albumin at a cell density equivalent to 2/3 fat pad/ml. Aliquots of cell suspension (1 ml) were incubated for 30 min under an atmosphere of 95 % O_2/5 % CO_2 in a final volume of 4 ml of KRB containing 1 % (w/v) defatted albumin, 5 mM glucose with AMPK activator compound dilutions (1000-fold from stocks in DMSO) to give the final concentrations indicated in the Figures. Control incubations contained 0.1% (v/v) DMSO as vehicle. For incubations with noradrenaline, aliquots of cell suspension (1 ml) were incubated in a final volume of 4 ml of KRB containing 3 % (w/v) defatted albumin, 4 mU/ml adenosine deaminase, 5 mM glucose with or without 30 µM SC4 + 0.1 mM AICA riboside for 15 min at 37 °C. The cells were then incubated for a further 30 min with the indicated concentrations of noradrenaline. Following incubation, the cells were harvested by centrifugation (200 g x 20 s) and freeze-stopped. For incubations with noradrenaline, incubation media were retained for glycerol assay as a measure of lipolysis [28]. Medium glycerol concentrations are expressed relative to LDH activity to correct for differences in amounts of cells used in each experiment. Freeze-stopped cells were homogenized in 0.5 ml of "Hepes sucrose buffer" (0.25 M sucrose, 1 mM EDTA, 1 mM EGTA, 20 mM NaF, 5 mM sodium pyrophosphate, 5 mM β-glycerol phosphate, 15 mM 2-mercaptoethanol, 20 mM Hepes, pH 7.4, and protease inhibitor cocktail (Roche)) on ice using an Ultra-Turrax tissue disintegrator. After centrifugation (20000 g x 5 min at 4°C, Eppendorf microfuge) the infranatants (full extracts) were removed and stored at -80°C prior to enzyme assay and immunoblotting. For cells incubated with noradrenaline with or without SC4 + AICA riboside, following homogenization/centrifugation, the infranatant was drawn off and the fat layer was removed from the tube and extracted by adding 200 µl of sucrose buffer containing 1 % (w/v) Triton X-100 and 50 µl of 5-fold concentrated SDS-PAGE Laemmli sample buffer. After heating at 95°C for 5 min

and centrifugation (2000 g x 5 min at 20°C, Eppendorf microfuge), an aliquot (30 µl) of supernatant was subjected to SDS-PAGE for immunoblotting.

Mouse epididymal fat pads were minced into pieces and pre-incubated pairwise in 4 ml of KRB buffer containing 1 % (w/v) defatted albumin with 10 µM SC4 + 0.1 mM AICA riboside or DMSO and 5 mM glucose for 15 min and then incubated for 60 min with or without insulin (0.1 µM). Following incubation, the fat pad pieces were separated from incubation media by flotation, freeze-stopped and homogenized in 0.5 ml of Hepes sucrose buffer for enzyme assay and immunoblotting as described above. In some experiments rates of lipogenesis were measured in epididymal fat pads from WT or WT versus AMPKα1 KO or WT versus ACC1/2 S79A/S212A double KI mice. The fat pads were harvested and weighed for normalization. The pads were then minced and pre-incubated pairwise in 4 ml of KRB buffer containing 1 % (w/v) defatted albumin and either 5 mM glucose, 5 mM glucose plus 5 mM sodium acetate or 5 mM glucose plus 0.5 mM palmitate with or without 10 µM SC4 + 0.1 mM AICA riboside. After 15 min, [U-^{14}C] glucose (20 dpm/nmol), [U-^{14}C] acetate (200 dpm/nmol) or [9,10-^{3}H(N)] palmitate (200 dpm/nmol) was added, respectively, and incubation was continued with or without insulin (0.1 µM). After 60 min, the fat pad pieces were collected by centrifugation (200 g x 20 s) and extracted with 1:2 (v/v) $CHCl_3$:CH_3OH for measurements of rates of lipogenesis/fatty acid esterification as described [29]. Epididymal fat pads from WT versus AMPKα1 KO mice were also weighed and preincubated with and without 10 µM SC4 + 0.1 mM AICA riboside for 15 min followed by incubation for 60 min with or without insulin (0.1 µM). Subsequently, [U-^{14}C] 2-deoxyglucose (200 dpm/nmol) and 0.1 mM non-radioactive 2-deoxyglucose were added for measurements of rates of glucose uptake essentially as described [30]. Fat pads from WT and AMPKα1 KO mice were incubated with 10 µM SC4 + 0.1 mM AICA riboside or DMSO and 5 mM glucose for 15 min and then incubated for 30 min with or without insulin (0.1 µM) for extraction and adenine nucleotide measurements as described [31].

Enzyme assays and nucleotide measurements

AMPK activity was measured following immunoprecipitation as described previously [19]. Briefly, full extracts from adipocytes or adipose tissue prepared in Hepes sucrose buffer (0.5 ml) were immunoprecipitated by mixing with anti-AMPKα1 + anti-AMPKα2 antibodies (0.5 µg of each per sample) coupled to Protein G Sepharose beads (50 µl per sample in PBS 1:1 vol/vol slurry) with agitation overnight at 4°C. AMPK was assayed in a final volume of 50 µl containing 0.1 mM [γ-^{32}P] ATP, 0.2 mM AMP and 200 µM AMARA peptide at 30°C. After 10 min, aliquots (5 µl) were taken and spotted onto P81 phosphocellulose papers for measurement of ^{32}P-incorporation by scintillation counting. LDH in full extracts of adipocytes and epididymal fat pads was assayed spectrophotometrically as described [28]. Mouse or rat epididymal fat pad extracts (75 µl) were assayed for total GPAT activity in a final volume of 0.5 ml 100 mM Hepes pH 7.4 containing 1.75 mg/ml defatted albumin, 1 mM dithiothreitol, 50 µM palmitoyl-CoA, 0.5 mM [2-^{3}H] *sn*-glycerol 3-phosphate (3000 dpm/nmol) at 30 °C. Some assays also included 10 mM N-ethylmaleimide (NEM) for mitochondrial GPAT assay [28]. After 10 min, the reactions were stopped with 2 ml of water-saturated butanol by vortexing. Butanol layers were washed for liquid scintillation counting as described [28]. GPAT activities are expressed relative to LDH activity to correct for differences in recovery and homogenization. For the preparation of [2-^{3}H] *sn*-glycerol 3-phosphate, [2-^{3}H] glycerol (0.5 mCi) in ethanol was vacuum dried for incubation in 1 ml of 100 mM Hepes pH 7.4 containing 1 mM non-radioactive

glycerol, 5 mM ATP.Mg and 5 Units of glycerol kinase overnight at 30 °C. After stopping with 0.5 ml 2 % (w/v) activated charcoal and centrifugation (5000 rpm x 3 min, Eppendorf microfuge) the supernatant was applied to a 1 ml Pasteur pipette column of Dowex 1X8-200 (chloride form) which was then washed with water and eluted sequentially with 2x 1 ml of 50 mM NaCl, 100 mM NaCl, 150 mM NaCl, 200 mM NaCl and 250 mM NaCl. Fractions containing radioactivity were stored frozen at -20 °C.

Immunoblotting

Equal volumes of sample (10-20 µl) were loaded into each well of polyacrylamide gels (7.5 % (w/v) for ACC and 12 % (w/v) for AMPK) for SDS-PAGE using separate gels for detection with anti-phospho- versus anti-total protein antibodies. Following SDS-PAGE and transfer, PVDF membranes were blocked in TBS-T buffer containing 5 % (w/v) non-fat dry milk in for 1 h. After washing with TBS-T (3 x 10 min), the membranes were incubated with primary antibodies (diluted as indicated under "Materials") in TBS-T containing 3 % (w/v) bovine serum albumin overnight at 4°C. The membranes were washed with TBS-T (3 x 10 min) and incubated with secondary antibodies (ab6789, ab6721, ab6900, Abcam) diluted 1:20000 or 1:50000 at room temperature. After washing three times with TBS-T, immunoreactive bands were detected with Immobilon® classico western HRP substrate (Millipore) for quantification by chemiluminescence scanning densitometry using the Fusion Solo S (Vilber) imaging system.

Other methods

The data are presented as means ± S.E.M. Statistical analysis was assessed by a Student's *t*-test in the software package “GraphPad Prism 5” and $P < 0.05$ was considered to be significant. One unit of protein kinase represents the amount that catalyses the phosphorylation of 1 nmol of substrate under the assay conditions. Otherwise, 1 unit of enzyme is the amount that catalyses the formation of 1 μmol of product under the conditions of the assay.

Data availability

All relevant data are contained within the main article and its supplementary files.

Results

Effects of small-molecule AMPK activators on AMPK activity along with AMPKα, ACC and Raptor phosphorylation in rat adipocytes

Effects of a panel of pharmacological AMPK activators in rat adipocytes incubated for 30 min were first compared by immunoprecipitating extracts with anti-AMPKα1 + anti-AMPKα2 antibodies to measure AMPK activity with the AMARA peptide as substrate in the presence of 0.2 mM AMP. Treatment with AICA riboside, 991 and O304 increased AMPKα1 + AMPKα2 activity, but incubation with 100 µM PF-739 and MK-8722 was without effect (Figure 1A). SC4 was the most effective AMPK activator in rat adipocytes eliciting a ~2.5-fold increase in AMPKα1 + AMPKα2 activity. AMPK activation measured in Figure 1A would be the result of increased AMPKα Thr172 phosphorylation plus allosteric stimulation by AMP, thus representing an increase in total AMPK activity. Indeed in the intact cell, immunoblotting of extracts revealed significantly increased AMPKα Thr172 phosphorylation in response to incubation with the AMPK activators except O304

(Figure 1B). Small but significant increases in downstream ACC Ser79 phosphorylation were observed in adipocytes incubated with AICA riboside, 991, SC4 and O304, as detected by immunoblotting, but basal ACC phosphorylation in the controls was high in spite of the fact that the animals had free access to food and were not starved (Figure 1C). Also, there were small but significant increases in downstream Raptor Ser792 phosphorylation in adipocytes incubated with all the AMPK activators except PF-739 (Figure 1D). In a separate series of experiments in which adipocytes were incubated with lower doses of PF-739 and MK-8722 (30 μM) along with the other activators at the same concentrations used in Figure 1, significant AMPKα1 + AMPKα2 activation was observed with all molecules and basal ACC phosphorylation was lower such that more pronounced effects of compound treatment to increase ACC phosphorylation were observed (Supplementary Figure S1).

Since SC4 was the most effective AMPK activator in rat adipocytes, we examined effects of increasing concentrations of SC4 with and without a submaximal dose of AICA riboside (0.1 mM) on AMPK activity, as studied previously for combined effects of AICA riboside and 991 in skeletal muscle [32]. SC4 treatment dose-dependently increased AMPK activity and AMPKα Thr172 phosphorylation, but again the increase in ACC Ser79 phosphorylation was modest (Figure 2). Incubation with 0.1 mM AICA riboside alone did not increase AMPKα1 + AMPKα2 activity or AMPKα Thr172 phosphorylation (Figure 2A,B). However, incubation with AICA riboside enhanced AMPKα Thr172 phosphorylation by SC4 at concentrations above 1 μM (Figure 2A,B) and at a concentration of 10 μM SC4, AMPKα1 + AMPKα2 activity reached similar levels to those seen with 100 μM SC4 alone (Figure 1A). Therefore, in subsequent experiments 0.1 mM AICA riboside was used in combination with submaximal doses of SC4 (10 μM or 30 μM) to achieve AMPK activation.

SC4 + AICA riboside inhibits noradrenaline-stimulated lipolysis in rat adipocytes

Incubation of rat adipocytes with noradrenaline in the presence of adenosine deaminase increased medium glycerol release as a measure of lipolysis dose-dependently with an EC50 value of 0.20 ± 0.11 μM (Fig. 3A). Preincubation with SC4 + AICA riboside inhibited lipolysis by ~40 % at 0.2 μM noradrenaline and increased the EC50 for noradrenaline by 70 % to a value of 0.34 ± 0.12 μM, $P<0.05$, paired *t*-test (Figure 3A). Following centrifugation of adipocyte extracts at 4°C, the fat layer, shown to contain triglyceride lipase activity and HSL protein [33], was removed and extracted for SDS-PAGE and immunoblotting (Figure 3B). AMPK activation by SC4 + AICA riboside was validated by immunoblotting the soluble fraction to verify that the treatment led to increased AMPKα Thr172 and increased ACC Ser79 phosphorylation which were also increased in incubations with noradrenaline (not shown). Incubation with noradrenaline dose-dependently increased HSL Ser563 and HSL Ser660 phosphorylation (Figure 3C,D). HSL Ser563 and Ser660 are sites phosphorylated by cyclic-3',5'-AMP (cAMP)-dependent protein kinase (PKA). Interestingly, incubation with SC4 + AICA riboside significantly reduced noradrenaline-induced HSL Ser563 phosphorylation up to a concentration of 0.3 μM noradrenaline without affecting the increase in HSL Ser660 phosphorylation induced by noradrenaline (Fig. 3C,D). Increasing concentrations of noradrenaline had no effect on HSL Ser565 phosphorylation (AMPK site) either in the absence or in the presence of SC4 + AICA riboside (Fig. 3E). Incubation with noradrenaline dose-

dependently increased ATGL Ser406 phosphorylation (Fig. 3F). Furthermore, incubation with SC4 + AICA riboside increased basal ATGL Ser406 that further increased in the presence of maximal doses of noradrenaline (Fig. 3F).

SC4 + AICA riboside inhibits insulin-stimulated lipogenesis from glucose and acetate in mouse fat pads

Mouse fat pads from WT mice were incubated pairwise with and without insulin with and without SC4 + AICA riboside. Incubation with insulin increased the rate of lipogenesis, a process that encompasses both fatty acid and TG synthesis, from radioactive glucose by ~2-fold (Supplementary Figure S2A). Incubation in the presence of SC4 + AICA riboside had no effect on basal lipogenesis but decreased insulin-stimulated lipogenesis from glucose by ~20 % but not back to basal values (Supplementary Figure S2A). Incubation of fat pads with insulin increased the rate of lipogenesis from radioactive acetate ~3-fold (Supplementary Figure S2B). Lipogenesis from acetate bypasses the provision of 2-carbon units by glycolysis and PDH but non-radioactive glucose was present to furnish *sn*-glycerol 3-phosphate for esterification. Incubation in the presence of SC4 + AICA riboside had no effect on basal lipogenesis from acetate but decreased insulin-stimulated lipogenesis from acetate by ~35 %, though again not back to basal values (Supplementary Figure S2B).

SC4 + AICA riboside treatment of mouse fat pads decreases insulin-stimulated lipogenesis from glucose or acetate in an AMPKα1-dependent manner

To test the potential involvement of AMPK activation in mediating the inhibition of insulin-stimulated lipogenesis, measurements of lipogenesis in fat pads from WT versus AMPKα1 KO mice were performed. In fat pads from both WT and AMPKα1 KO mice, incubation with insulin increased the rates of lipogenesis from glucose and acetate by ~2 to 3-fold (Figure 4A,B). Treatment of fat pads from WT mice with SC4 + AICA riboside decreased insulin-stimulated lipogenesis from glucose or acetate by ~30 % and ~25 %, respectively, but these effects were lost in incubated fat pads from AMPKα1 KO mice (Figure 4A,B) suggesting that the effects were AMPKα1-dependent. In parallel incubations of fat pads from WT mice, incubation with insulin decreased AMPKα Thr172 phosphorylation, as observed previously in rat adipocytes [34], and in the presence of insulin, treatment with SC4 + AICA riboside increased AMPKα Thr172 phosphorylation (Figure 3C). These effects were strongly ablated in incubated fat pads from AMPKα1 KO mice (Figure 4C). Nevertheless, increased ACC phosphorylation by SC4 + AICA riboside treatment was still seen in the presence of insulin in fat pads from AMPKα1 KO mice (Figure 4D). ACC is known to be an extremely good AMPK substrate such that signals in immunoblots probed with sensitive commercial anti-phospho ACC antibodies become saturated and a small amount of residual AMPKα1 in the KO activated by SC4 + AICA riboside in the presence of insulin (see below, Figure 5C) would be enough to see increased ACC phosphorylation. The effect could also have been due to compensating AMPKα2 activation by SC4 + AICA riboside in the presence of insulin (see below, Figure 5D). It is noteworthy in this respect that AMPK knockdown by transfecting rat adipocytes with a dominant-negative form of AMPK did not completely suppress ACC phosphorylation in response to AICA riboside treatment, even though AMPK activation was impaired [2]. Raptor is a poorer AMPK substrate than ACC and the effect of SC4 + AICA riboside treatment to increase the phosphorylation of Raptor in fat pads from WT mice incubated with insulin was more markedly reduced in

incubated fat pads from AMPKα1 KO mice (Figure 4E) but might also have been phosphorylated by compensating AMPKα2 activation by SC4 + AICA riboside. In summary, the fact that inhibition of lipogenesis from glucose or acetate by SC4 + AICA riboside was lost in in fat pads from AMPKα1 KO mice suggests that this effect is AMPKα1-dependent and phosphorylation of ACC and Raptor seen in in incubated fat pads from AMPKα1 KO mice was probably due to residual AMPKα1 or compensating AMPKα2 (see below).

Effects of AMPKα1 KO on AMPKα1 and AMPKα2 protein content and AMPKα1 and AMPKα2 activities in mouse fat pads

Extracts prepared from fat pads of WT and AMPKα1 KO mice incubated with and without insulin with and without SC4 + AICA riboside were immunoblotted with anti-AMPKα1 and anti-AMPKα2 antibodies and assayed for AMPKα1 and AMPKα2 activity. The protein level of AMPKα1 was decreased by ~90 % in extracts from AMPKα1 KO versus WT mice (Figure 5A) whereas the level of AMPKα2 increased by 50 % (Figure 5B). In fat pads from AMPKα1 mice, AMPKα1 activity was markedly less than in fat pads from WT mice (Figure 5C). In fat pads from WT mice, AMPKα2 activity was much less than AMPKα1 activity but AMPKα2 activity increased in fat pads that had been incubated with SC4 + AICA riboside (Figure 5D). Thus, despite of the 50 % compensatory increase in AMPKα2 protein levels in fat pads from AMPKα1 KO versus WT mice, AMPKα2 activity from AMPKα1 KO mice would be about 25 % of total AMPK activity in fat pads from WT mice in the SC4 + AICA riboside stimulated condition.

SC4 + AICA riboside treatment of mouse fat pads decreases insulin-stimulated lipogenesis via AMPK-induced phosphorylation of ACC

To determine whether insulin-stimulated lipogenesis was inhibited via AMPK-induced phosphorylation of ACC, lipogenesis from radioactive acetate was measured in fat pads from WT versus ACC1/2 S79A/S212A double KI mice. Insulin increased the rate of lipogenesis from radioactive acetate ~2-fold (Figure 6A). Moreover, insulin-stimulated rates of lipogenesis from acetate were increased in incubated fat pads from ACC1/2 S79A/S212A KI versus WT mice (Figure 6A), indicating that the removal of the ACC inactivating phosphorylation sites in WAT increases lipogenesis as seen in hepatocytes from ACC1/2 S79A/S212A KI mice [26]. Also, the effect of insulin to increase lipogenesis was maintained in incubated fat pads from ACC1/2 S79A/S212A KI, as observed previously [29]. Importantly, the effect of SC4 + AICA riboside treatment to inhibit insulin-stimulated lipogenesis from radioactive acetate was lost in fat pads from ACC1/2 S79A/S212A KI mice (Figure 6A), suggesting that ACC is the key AMPK target phosphorylated by AMPK to explain reduced insulin-stimulated lipogenesis. In fat pads from WT mice, treatment with insulin decreased ACC Ser79 phosphorylation, an effect potentially involving AMPKα1 inhibition via PKB as described previously [29,34,35], but incubation with SC4 + AICA riboside in the presence of insulin resulted in increased ACC phosphorylation (Figure 6B). ACC phosphorylation was not detectable in incubated fat pads from ACC1/2 S79A/S212A KI mice, as expected (Figure 6B).

The effect of SC4 + AICA riboside treatment to inhibit insulin-stimulated glucose uptake persists in fat pads from AMPKα1 KO mice

Effects of AMPK activation by SC4 + AICA riboside treatment on glucose uptake were investigated in fat pads from WT versus AMPKα1 KO mice. Incubation of fat

pads with insulin increased the rate of radioactive 2-deoxyglucose uptake ~2-fold (Figure 7A). Incubation with SC4 + AICA riboside had no effect on basal 2-deoxyglucose uptake but decreased insulin-stimulated 2-deoxyglucose uptake by ~50 % back to basal values (Figure 7A). However, the effect of SC4 + AICA riboside to decrease insulin-stimulated 2-deoxyglucose uptake was still apparent in fat pads from AMPKα1 KO mice (Figure 7B), suggesting that the effect was partly AMPKα1-independent.

Effects of SC4 + AICA riboside treatment on insulin targets in fat pads from WT mice and rats

The fact that the effect of SC4 + AICA riboside treatment to inhibit insulin-stimulated lipogenesis from radioactive acetate was lost in fat pads from ACC1/2 S79A/S212A KI mice suggests that there are no control points for AMPK beyond ACC in the lipogenic pathway, but control upstream of ACC cannot be excluded. Therefore, effects of SC4 + AICA riboside on insulin targets upstream of ACC potentially involved in controlling the lipogenic pathway from glucose were studied by immunoblotting full extracts from incubated fat pads. These targets are PKB, TBC1D4, ACL and PDH. Firstly, incubation with insulin increased PKB Ser473 and PKB Thr308 phosphorylation in fat pads from WT mice (Figure 8A, B) and increased PKB Ser473 phosphorylation in rat fat pads (Supplementary Figure S3A). However, increased PKB phosphorylation was unaffected by SC4 + AICA riboside treatment. Also, SC4 + AICA riboside treatment increased AMPKα Thr172 and ACC Ser79 phosphorylation both in fat pads from WT mice (Figure 8C,D) and in rat fat pads (Supplementary Figure S3B,C) and increased AMPK and ACC phosphorylation by SC4 + AICA riboside was seen the presence of insulin. Insulin-stimulated glucose uptake in adipocytes can partly be explained by increased TBC1D4 phosphorylation mediated by PKB [36] and TBC1D4 Thr642 is one of the PKB sites implicated in insulin-stimulated GLUT4 translocation [37]. Incubation of mouse fat pads with insulin increased TBC1D4 Thr642 phosphorylation and, in the presence of SC4 + AICA riboside, insulin-stimulated TBC1D4 Thr642 phosphorylation tended to decrease (Figure 8E). ACL is a key lipogenic enzyme phosphorylated by insulin in rat adipocytes via PKB at Ser454 [38] (Ser455 in mouse), but its role in the control of lipogenesis is an enigma as there appears to be no effect on enzyme activity. Incubation of mouse fat pads with insulin increased ACL Ser455 phosphorylation and, in the presence of SC4 + AICA riboside, insulin-stimulated ACL phosphorylation decreased by ~25 % (Figure 8F). PDH is activated by insulin in adipose tissue via dephosphorylation of Ser293 (site 1) and Ser300 (site 2) [39,40]. In incubated rat fat pads, SC4 + AICA riboside treatment had no effect on basal PDH E1α Ser293 and Ser300 phosphorylation and PDH E1α Ser293 and Ser300 dephosphorylation by insulin was still apparent in the presence of SC4 + AICA riboside (Supplementary Figure S3D,E).

SC4 + AICA riboside treatment has no effect on fatty acid esterification or GPAT activity in fat pads from WT mice

Incubation of mouse fat pads with insulin increased rate of esterification from radioactive palmitate by ~2-fold (Figure 9A). Incubation with SC4 + AICA riboside had no effect on the rate of palmitate esterification either in the basal or insulin-stimulated conditions (Figure 9A). Moreover, treatment with SC4 + AICA riboside had no effect on the total activity of GPAT, a key regulatory enzyme of the

esterification pathway [41], either under basal conditions or in the presence of insulin (Figure 9B). The measurements of total GPAT activity were made on full extracts taken from the experiment shown in Figure 8 indicating insulin-induced PKB phosphorylation (Figure 8A,B) and AMPK activation by SC4 + AICA riboside (Figure 8C,D). Likewise there was no effect of either insulin or SC4 + AICA riboside either alone or in combination on total GPAT activity in extracts from incubated rat fat pads (Supplementary Figure S3F) with appropriate controls for effects of insulin (Supplementary Figure S3A) and SC4 + AICA riboside (Supplementary Figure S3B,C). Total GPAT activity in extracts comprises microsomal (NEM-sensitive) and mitochondrial (NEM-insensitive) GPAT activities [28]. However in rat fat pads, NEM-insensitive GPAT activity was very low (about 10 % of NEM-sensitive GPAT) and SC4 + AICA riboside treatment had no effect on NEM-insensitive GPAT activity (not shown).

Discussion

Screening of a panel of small-molecule AMPK activators in incubated rat adipocytes indicated that SC4 was the most effective in inducing stable AMPK activation (Figure 1A, Supplementary Figure S1A). SC4 is considered as a pan β direct AMPK activator [18], and shows some selectivity *in vitro* for AMPKα2-containing complexes [22]. However SC4 does activate AMPKα1β1γ1 with an EC_{50} 3-times lower than for AMPKα2β2γ1 *in vitro* [22]. Concerning AMPK isoform expression in WAT, AMPKα1 protein predominates in rat and mouse, AMPKβ1 protein predominates in rat, AMPKβ1 and AMPKβ2 proteins are expressed roughly equally in mouse and humans [4] and AMPKγ1 mRNA is expressed in humans (https://www.proteinatlas.org/). In the presence of 0.1 mM AICA riboside, which alone did not activate AMPK, AMPK activation by a submaximal dose of SC4 (10 μM) was enhanced (Figure 2). Indeed, synergy of AMPK activation has been demonstrated for AICA riboside in combination with 991 [32] and for drug/ligand effects via binding to the AMPKγ and AMPKβ subunits [42,43]. Therefore, a combination of submaximal concentrations of both AICA riboside (0.1 mM) and SC4 (10 or 30 μM) was used to investigate effects of specific pan-β AMPK activation on metabolic parameters in rodent WAT.

Preincubation of rat adipocytes with SC4 + AICA riboside inhibited lipolysis induced by 0.2 μM noradrenaline by ~40 %, causing a right shift in the dose curve (Figure 3A) and increasing the EC50 for noradrenaline by ~70 %. Also, preincubation of fat pads from WT mice with 30 μM SC4 + 0.1 mM AICA riboside inhibited lipolysis induced by 1 μM noradrenaline by ~35 % (data not shown). Concerning the mechanism by which SC4 + AICA riboside treatment inhibited noradrenaline-induced lipolysis, surprisingly there was no significant effect on the level of HSL Ser565 phosphorylation either in the absence or presence of increasing concentrations of noradrenaline (Figure 3E), in spite of the presumption that phosphorylation at this site mediates the anti-lipolytic effect of AMPK [2,8]. Incubation of rat adipocytes with increasing concentrations of noradrenaline increased HSL Ser660 phosphorylation that was unaffected by SC4 + AICA riboside treatment (Figure 3D). HSL Ser660 is one of two PKA sites whose phosphorylation plays a major role in HSL activation and translocation [44]. Incubation of rat adipocytes with increasing concentrations of noradrenaline also increased HSL Ser563 phosphorylation that was inhibited by SC4 + AICA riboside treatment at a submaximal concentration of 0.3 μM noradrenaline

(Figure 3C). HSL Ser563 is also a PKA site but its precise role is unclear [44]. Unlike in hepatocytes where AMPK activation by 991 reduced glucagon-induced increases in cAMP by activating a cyclic nucleotide phosphodiesterase [45], in rat adipocytes we did not see any effects upon incubation with 100 μM 991 on increases in cAMP levels induced by 1 μM noradrenaline (data not shown). Therefore, the effect of AMPK activation to reduce the increase in HSL Ser563 phosphorylation at the submaximal dose of 0.3 μM noradrenaline (Figure 3C), without affecting HSL Ser660 phosphorylation (Figure 3E), might have been due to activation of a phosphoprotein phosphatase specific for the HSL Ser563 site. Based on the use of AMPKα1 knockout mice, the effect of AICA riboside to inhibit β-agonist–stimulated lipolysis in WAT was shown to be AMPK-dependent [2]. In conclusion, SC4 + AICA riboside treatment inhibited noradrenaline-induced lipolysis, possibly involving reduced HSL Ser563 phosphorylation.

AMPK activation has been proposed to have a pro-lipolytic effect by activating ATGL via Ser406 phosphorylation [9]. Interestingly, this site is also a PKA site and increased lipolysis was associated with increased ATGL phosphorylation in mouse and human adipose tissue [46]. However, in human adipose tissue, AMPK activation by incubation with AICA riboside did not lead to increased ATGL Ser404 phosphorylation (the equivalent site in mouse ATGL Ser406) [46]. In the present study, incubation of rat adipocytes with increasing concentrations of noradrenaline led to a dose-dependent increase in ATGL Ser406 phosphorylation (Figure 3F). Incubation with SC4 + AICA riboside increased basal ATGL Ser406 phosphorylation that further increased in the presence of maximal doses of noradrenaline (Figure 3F). Therefore, ATGL Ser406 phosphorylation might well participate in the stimulation of lipolysis by noradrenaline in WAT. However, basal rates of lipolysis were unaffected by treatment with SC4 + AICA riboside (Figure 3A) in spite of increased ATGL Ser406 phosphorylation (Figure 3F). One possibility is that other AMPK sites in ATGL could antagonize the activating effect of Ser406 phosphorylation.

In incubated mouse fat pads, insulin stimulated lipogenesis from glucose and acetate, and this effect was inhibited by SC4 + AICA riboside treatment (Supplementary Figure S2A,B, Figure 4A,B). Moreover, with glucose or acetate as substrate, the effect of SC4 + AICA riboside treatment to reduce insulin-stimulated lipogenesis was lost in incubated fat pads from AMPKα1 KO versus WT mice (Figure 4A,B), suggesting that the effect was AMPKα1-dependent. In incubated fat pads from ACC1/2 S79A/S212A double KI versus WT mice, the effect SC4 + AICA riboside treatment to inhibit insulin-stimulated lipogenesis from radioactive acetate was completely lost (Figure 6A). These results pinpoint ACC phosphorylation as the principal site to explain the effect of AMPK activation to inhibit insulin-stimulated lipogenesis and suggest that there are no other control points for AMPK in the lipogenic pathway (fatty acid + TG synthesis) beyond ACC (see below). The data also suggest that despite the fact that SC4 + AICA riboside treatment inhibited glucose uptake, this would not be limiting for providing *sn*-glycerol 3-phosphate for lipogenesis from acetate in fat pads from ACC1/2 S79A/S212A double KI mice. Other sites of control by AMPK upstream of ACC in the lipogenic pathway cannot be excluded. Potential control points in the conversion of glucose to TG include glucose transport, PDH and ACL. Indeed, insulin-stimulated glucose uptake was inhibited by SC4 + AICA riboside treatment of mouse fat pads (Figure 7A). However, the inhibition of insulin-stimulated glucose transport was still apparent in fat pads from AMPKα1 KO mice incubated with SC4 + AICA riboside (Figure 7B), suggesting that

the effect was partly AMPKα1-independent. The inhibition of insulin-stimulated glucose uptake by SC4 + AICA riboside in fat pads from AMPKα1 KO mice could have been due to an off-target effect of compound treatment or compensation by AMPKα2 (Figure 5). SC4 + AICA riboside treatment had no effect on intracellular ATP concentrations nor on the adenylate energy charge (AEC) calculated from ATP, ADP and AMP levels in mouse fat pads from WT and AMPKα1 KO mice, suggesting that cell viability/activity was not compromised by SC4 + AICA riboside treatment to explain the inhibition of lipogenesis/glucose uptake and that AMPKα1 KO would not sustain cell viability (Supplementary Figure S4). Our results are somewhat at variance with recent findings where use of AMPKβ1 S108A expressing adipocytes, in which AMPK activation by A-769662 was impaired, suggested that the inhibition of insulin-stimulated glucose uptake by A-769662 was AMPK-independent [10]. Regarding mechanisms by which AMPK activation could inhibit insulin-stimulated lipogenesis from from glucose upstream of ACC, incubation of fat pads with SC4 + AICA riboside tended to reduce the insulin-induced increases in TBC1D4 Thr642 and decreased insulin-induced ACL Ser455 phosphorylation (Figure 8E,F), whereas PDH E1α Ser293 and Ser300 dephosphorylation by insulin was seemingly unaffected (Supplementary Figure S3D,E). TBC1D4 Thr642 and ACL Ser455 are recognized PKB sites, but surprisingly incubation with SC4 + AICA riboside had no effect on insulin-induced increases in PKB Ser473 (Figure 8A, supplementary Figure S3A) or increased PKB Thr308 phosphorylation (Figure 8B). Our findings are in agreement with [10] where AICA riboside or A-769622 treatment of adipocytes had no effect on insulin-induced PKB Ser473 phosphorylation. However in these studies, AICA riboside or A-769622 treatment had no effect on insulin-stimulated TBC1D4 Thr642 phosphorylation whereas in our hands treatment with SC4 + AICA riboside tended to reduce insulin-induced TBC1D4 phosphorylation (Figure 8E). The lack of effect of SC4 + AICA riboside treatment on insulin-induced PKB phosphorylation suggests that reduced insulin-induced TBC1D4 Thr642 and ACL Ser455 phosphorylation might have been due to AMPK-induced activation of a phosphoprotein phosphatase that dephosphorylates these sites. Incubation of mouse fat pads with SC4 + AICA riboside had no effect on basal or insulin-stimulated esterification from radioactive palmitate (Fig. 9A). Moreover, total GPAT activity was unaffected by incubation with either insulin or SC4 + AICAR alone or in combination (Figure 9B, Supplementary Figure S3F). AICA riboside treatment was proposed to inactivate liver mitochondrial GPAT [11]. However direct phosphorylation and phosphorylation site determination were never reported. On the other hand, microsomal GPAT3 phosphorylation on Ser68 was detected in a phosphoproteomic screen of human muscle during exercise [47]. Although microsomal GPAT3 Ser68 lies in a favourable consensus for phosphorylation by AMPK (SILKNSApS^{68}VGIIQRD), our findings do not support control of GPAT activity as a result of AMPK activation.

Pharmacological AMPK activation is recognized as a novel approach for treating type 2 diabetes [48]. Since AMPK activation promotes insulin-independent glucose uptake in skeletal muscle, drugs that specifically activate AMPK in this tissue would be most beneficial, possibly in combination with metformin, which acts primarily on the liver to reduce glucose production. However, tissue-specific AMPK activation in muscle might not be possible and so positive and negative effects of whole-body AMPK activation need to be considered. *In vivo* administration of pan-AMPK activators PF-739 [23] and MK-8722 [24] that bind to the ADaM site or administration of pan-AMPK activator O304 [25] improved glucose tolerance in

insulin-resistance rodent models. Long-term use of MK-8722 was associated with cardiac hypertrophy that was reminiscent of that seen in human athletes, and thus might not be a serious complication [24].

AMPK activation by SC4 + AICA riboside treatment in rat adipocytes inhibited β-agonist-stimulated lipolysis without affecting basal lipolysis (Figure 3A). This could be beneficial *in vivo* by reducing circulating free fatty acids linked to the development of insulin resistance, particularly in skeletal muscle [5], but without leading to TG accumulation in WAT that might result if lipolysis was completely blocked by AMPK activation. Although AMPK activation in human primary adipocytes did not inhibit β-agonist-stimulated lipolysis [4], this conclusion was based on the use of 991, which we show is not the most effective AMPK activator, at least in rat adipocytes (Figure 1). The storage capacity of WAT is limited and once surpassed, fat accumulates in ectopic tissues (such as skeletal muscle, liver and heart), a phenomenon called "lipotoxicity" that leads to insulin resistance [49]. The effects of AMPK activation to inhibit insulin-stimulated glucose uptake and insulin-stimulated *de novo* lipogenesis in WAT could thus be beneficial by reducing TG content. It should be mentioned that *de novo* lipogenesis in human WAT can have an insulin sensitizing effect [50]. However, reduced TG storage in WAT could counteract the development of insulin resistance in other tissues by lowering circulating free fatty acids.

Funding

The work was funded by the Fund for Medical Scientific Research (FNRS, Belgium) grant numbers T.0008.15 and T.0208.20. GRS is supported by a Canada Research Chair and the J Bruce Duncan Endowed Chair in Metabolic Diseases and program grants from the Canadian Institutes of Health Research (201709FDN-CEBA-116200) and Diabetes Canada (DI-5-17-5302-GS). BEK is supported by the National Health and Medical Research Council of Australia and by the Australian Research Council (NHMRC, APP1085460 & DP170101196).

Author contributions

S.-J.C. carried out experiments on fat pads and adipocytes and performed enzyme assays, immunoblotting and data analysis. M.J. was involved in supervision and interpretation of data. S.P.D.R. supervised improved immunoblot analysis. G.R.S. and B.E.K. generated and provided ACC1/2 S79A/S212A KI mice. B.V. generated and provided AMPKα1 KO mice. M.H.R. was involved in conception, design, interpretation of data and drafted the article.

Competing interests

G.R.S. has received research funding from Esperion Therapeutics, Espervita Therapeutics, Poxel Pharmaceuticals and Novo Nordisk, honoraria and/or consulting fees from Astra Zeneca, Eli-Lilly, Esperion Therapeutics, Poxel Pharmaceuticals, Merck and is a founder and shareholder of Espervita Therapeutics.

References

1. Hardie, D.G., Ross, F.A., and Hawley, S.A. (2012) AMPK: a nutrient and energy sensor that maintains energy homeostasis. Nat. Rev. Mol Cell. Biol. **13**, 251-262

2. Daval, M., Diot-Dupuy, F., Bazin, R., Hainault, I., Viollet, B., Vaulont, S., Hajduch, E., Ferré, P. and Foufelle, F. (2005) Anti-lipolytic action of AMP-activated protein kinase in rodent adipocytes. J. Biol. Chem. **280**, 25250-25257
3. Gauthier, M.-S., Miyoshi, H., Souza, S.C., Cacicedo, J.M., Saha, A.K., Greenberg, A.S. and Ruderman, N.B. (2008) AMP-activated protein kinase is activated as a consequence of lipolysis in the adipocyte: potential mechanism and physiological relevance. J. Biol. Chem. **283**, 16514-16524
4. Kopietz, F., Berggreen, C., Larsson, S., Säll, J., Ekelund, M., Sakamoto, K., Degerman, E., Holm, C. and Göransson, O. (2018) AMPK activation by A-769662 and 991 does not affect catecholamine-induced lipolysis in human adipocytes. Am. J. Physiol. Endocrinol. Metab. **315**, E1075-E1085
5. Mottillo, E.P., Desjardins, E.M., Crane, J.D., Smith, B.K., Green, A.E., Ducommun, S., Henriksen, T.I., Rebalka, I.A., Razi, A., Sakamoto, K., Scheele, C., Kemp, B.E., Hawke, T.J., Ortega, J., Granneman, J.G. and Steinberg, G.R. (2016) Lack of adipocyte AMPK exacerbates insulin resistance and hepatic steatosis through brown and beige adipose tissue function. Cell Metab. **24**, 118-129
6. Bijland, S., Mancini, S.J. and Salt, I.P. (2013) Role of AMP-activated protein kinase in adipose tissue metabolism and inflammation. Clin. Sci. (Lond). **124**, 491-507
7. Sullivan, J.E., Brocklehurst, K.J., Marley, A.E., Carey, F., Carling, D. and Beri, R.K. (1994) Inhibition of lipolysis and lipogenesis in isolated rat adipocytes with AICAR, a cell-permeable activator of AMP-activated protein kinase. FEBS Lett. **353**, 33-36
8. Garton, A.J., Campbell, D.G., Carling, D., Hardie, D.G., Colbran, R.J. and Yeaman, S.J. (1989) Phosphorylation of bovine hormone-sensitive lipase by the AMP-activated protein kinase. A possible antilipolytic mechanism. Eur. J. Biochem. **179**, 249-254
9. Kim, S.J., Tang, T., Abbott, M., Viscarra, J.A., Wang, Y. and Sul H.S. (2016) AMPK Phosphorylates Desnutrin/ATGL and Hormone-Sensitive Lipase To Regulate Lipolysis and Fatty Acid Oxidation within Adipose Tissue. Mol. Cell. Biol. **36**,1961-1976
10. Kopietz, F., Alshuweishi, Y., Bijland, S., Alghamdi, F., Dergerman, E., Sakamoto, K., Salt, I.P and Göransson, O. (2021) A-769662 inhibits adipocyte glucose uptake in an AMP-independent manner. Biochem. J. **478**, 633-646
11. Muoio, D.M., Seefeld, K., Witters, L.A. and Coleman, R.A. (1999) AMP-activated kinase reciprocally regulates triacylglycerol synthesis and fatty acid oxidation in liver and muscle: evidence that sn-glycerol-3-phosphate acyltransferase is a novel target. Biochem J. **338**, 783-791
12. Corton, J.M., Gillespie, J.G., Hawley, S.A. and Hardie, D.G. (1995) 5-aminoimidazole-4-carboxamide ribonucleoside. A specific method for activating AMP-activated protein kinase in intact cells? Eur. J. Biochem. **229**, 558–565
13. Cool, B., Zinker, B., Chiou, W., Kifle, L., Cao, N., Perham, M., Dickinson, R., Adler, A., Gagne, G., Iyengar, R., Zhao, G., Marsh, K., Kym, P., Jung, P., Camp, H. S. and Frevert, E. (2006) Identification and characterization of a small molecule AMPK activator that treats key components of type 2 diabetes and the metabolic syndrome. Cell Metab. **3**, 403–416
14. Sanders, M.J., Ali, Z.S., Hegarty, B.D., Heath, R., Snowden, M.A. and Carling, D. (2007) Defining the mechanism of activation of AMP-activated protein kinase

by the small molecule A-769662, a member of the thienopyridone family. J. Biol. Chem. **282**, 32539–32548
15. Göransson, O., McBride, A., Hawley, S.A., Ross, F.A., Shpiro, N., Foretz, M., Viollet, B., Hardie, D.G. and Sakamoto, K. (2007) Mechanism of action of A-769662, a valuable tool for activation of AMP-activated protein kinase. J. Biol. Chem. **282**, 32549–32560
16. Scott, J.W., van Denderen, B.J., Jorgensen, S.B., Honeyman, J.E, Steinberg, G.R., Oakhill, J.S., Iseli, T.J., Koay, A., Gooley, P.R., Stapleton, D. and Kemp, B.E. (2008) Thienopyridone drugs are selective activators of AMP-activated protein kinase beta1-containing complexes. Chem. Biol. **15**,1220-1230
17. Xiao, B., Sanders, M.J., Carmena, D., Bright, N.J., Haire, L.F., Underwood, E., Patel, B.R., Heath, R.B., Walker, P.A., Hallen, S., Giordanetto, F., Martin, S.R., Carling, D. and Gamblin, S.J. (2013) Structural basis of AMPK regulation by small molecule activators. Nature Commun. **4,** 3017
18. Steinberg, G.R. and Carling, D. (2019) AMP-activated protein kinase: the current landscape for drug development. Nat. Rev. Drug Discov. **18**, 527-551
19. Lai, Y.C., Kviklyte, S., Vertommen, D., Lantier, L., Foretz, M., Viollet, B., Hallén, S. and Rider, M.H. (2014) A small-molecule benzimidazole derivative that potently activates AMPK to increase glucose transport in skeletal muscle: comparison with effects of contraction and other AMPK activators. Biochem. J. **460,** 363–375
20. Hawley, S.A., Fullerton, M.D., Ross, F.A., Schertzer, J.D., Chevtzoff, C., Walker, K.J., Peggie, M.W., Zibrova, D., Green, K.A., Mustard, K.J., Kemp, B.E., Sakamoto, K., Steinberg, G.R. and Hardie, D.G. (2012) The ancient drug salicylate directly activates AMP-activated protein kinase. Science **336,** 918–922
21. Langendorf, C.G. and Kemp, B.E., (2015) Choreography of AMPK activation. Cell Res. **25**, 5-6
22. Ngoei, K., Langendorf, C.G., Ling, N., Hoque, A., Varghese, S., Camerino, M. A., Walker, S.R., Bozikis, Y.E., Dite, T.A., Ovens, A.J., Smiles, W.J., Jacobs, R., Huang, H., Parker, M.W., Scott, J.W., Rider, M.H., Foitzik, R.C., Kemp, B.E., Baell, J.B. and Oakhill, J.S. (2018) Structural Determinants for Small-Molecule Activation of Skeletal Muscle AMPK α2β2γ1 by the Glucose Importagog SC4. Cell Chem. Biol. **25,** 728–737.e9
23. Cokorinos, E.C., Delmore, J., Reyes, A.R., Albuquerque, B., Kjøbsted, R., Jørgensen, N.O., Tran, J.L., Jatkar, A., Cialdea, K., Esquejo, R.M., Meissen, J., Calabrese, M.F., Cordes, J., Moccia, R., Tess, D., Salatto, C.T., Coskran, T.M., Opsahl, A.C., Flynn, D., Blatnik, M., Li, W, Kindt, E, Foretz, M, Viollet, B, Ward, J, Kurumbail, R.G., Kalgutkar, A.S., Wojtaszewski, J.F.P., Cameron, K.O. and Miller, R.A. (2017) Activation of Skeletal Muscle AMPK Promotes Glucose Disposal and Glucose Lowering in Non-human Primates and Mice. Cell Metab. **25,** 1147–1159.e10
24. Myers, R.W., Guan, H.P., Ehrhart, J., Petrov, A., Prahalada, S., Tozzo, E., Yang, X., Kurtz, M.M., Trujillo, M., Gonzalez Trotter, D., Feng, D., Xu, S., Eiermann, G., Holahan, M.A., Rubins, D., Conarello, S., Niu, X., Souza, S.C., Miller, C., Liu, J., Lu, K., Feng, W., Li, Y., Painter, R.E., Milligan, J.A., He, H., Liu, F., Ogawa, A., Wisniewski, D., Rohm, R.J., Wang, L., Bunzel, M., Qian, Y., Zhu, W., Wang, H., Bennet, B., LaFranco Scheuch, L., Fernandez, G.E., Li, C., Klimas, M., Zhou, G., van Heek, M., Biftu, T., Weber, A., Kelley, D.E., Thornberry, N., Erion, M.D., Kemp, D.M. and Sebhat IK. (2017) Systemic pan-

AMPK activator MK-8722 improves glucose homeostasis but induces cardiac hypertrophy. Science **357,** 507–511
25. Steneberg, P., Lindahl, E., Dahl, U., Lidh, E., Straseviciene, J., Backlund, F., Kjellkvist, E., Berggren, E., Lundberg, I., Bergqvist, I., Ericsson, M., Eriksson, B., Linde, K., Westman, J., Edlund, T. and Edlund, H. (2018) PAN-AMPK activator O304 improves glucose homeostasis and microvascular perfusion in mice and type 2 diabetes patients. JCI Insight **3,** e99114
26. Fullerton, M.D., Galic, S., Marcinko, K., Sikkema, S., Pulinilkunnil, T., Chen, Z.P., O'Neill, H.M., Ford, R.J., Palanivel, R., O'Brien, M., Hardie, D.G., Macaulay, S.L., Schertzer, J.D., Dyck, J.R., van Denderen, B.J., Kemp, B.E. and Steinberg, G.R. (2013) Single phosphorylation sites in Acc1 and Acc2 regulate lipid homeostasis and the insulin-sensitizing effects of metformin. Nature Med. **19,** 1649–1654
27. Jørgensen, S.B., Viollet, B., Andreelli, F., Frøsig, C., Birk, J.B., Schjerling, P., Vaulont, S., Richter, E.A. and Wojtaszewski, J.F. (2004) Knockout of the alpha2 but not alpha1 5'-AMP-activated protein kinase isoform abolishes 5-aminoimidazole-4-carboxamide-1-beta-4-ribofuranosidebut not contraction-induced glucose uptake in skeletal muscle. J. Biol. Chem. **279,** 1070–1079
28. Rider, M.H. and Saggerson, E.D. (1983) Regulation by noradrenaline of the mitochondrial and microsomal forms of glycerol phosphate acyltransferase in rat adipocytes. Biochem. J. **214,** 235–246
29. Hussain, N., Chuang, S.J., Johanns, M., Vertommen, D., Steinberg, G.R., Kemp, B.E. and Rider, M.H. (2020) Effects of PKB/AKT inhibitors on insulin-stimulated lipogenesis and phosphorylation state of lipogenic enzymes in white adipose tissue. Biochem. J. **477**, 1373-1389
30. Chen, S., Zhao, Z., Ke, L., Li, Z., Li, W., Zhang, Z., Zhou, Y., Feng, X. and Zhu, W. (2018) Resveratrol improves glucose uptake in insulin-resistant adipocytes via Sirt1. J. Nutr. Biochem. **55,** 209–218
31. Johanns, M., Kviklyte, S., Chuang, S.-J., Corbeels, K., Jacobs, K., Herinckx, G., Vertommen, D., Schakman, O., Duparc, T., Cani, P.D., Bouzin, C., Andersén, H., Bohlooy-Y, M., Van der Schueren, B., Oscarsson, J. and Rider, M.H. (2019) Genetic deletion of soluble 5'-nucleotidase II reduces body weight gain and insulin resistance induced by a high-fat diet. Mol. Genet. Metab. **126**, 377-387
32. Bultot, L., Jensen, T.E., Lai, Y.-C., Madsen, A.L., Collodet, C., Kviklyte, S., Deak, M., Yavari, A., Foretz, M., Ghaffari, S., Bellahcene, M., Ashrafian, H., Rider, M.H., Richter, E.A. and Sakamoto, K. (2016) Benzimidazole derivative small-molecule 991 enhances AMPK activity and glucose uptake induced by AICAR or contraction in skeleal muscle. Am. J. Physiol. Endocrinol. Metab. **311,** E706–E719
33. Morimoto, C., Sumiyoshi, M., Kameda, K., Tsujita, T. and Okuda, H. (1999) relationship between hormone-sensitive lipolysis and lipase activity in rat fat cells. J. Biochem. **125**, 976-981
34. Kopietz F., Rupar K., Berggreen C., Säll J., Vertommen D., Degerman E., Rider M.H., Göransson O. (2020) Inhibition of AMPK activity in response to insulin in adipocytes - involvement of AMPK pS485, PDEs and cellular energy levels. Am. J. Physiol. Endocrinol. Metab. **319**, E459-E471
35. Berggreen, C., Gormand, A., Omar, B., Degerman, E. and Goransson, O. (2009) Protein kinase B activity is required for the effects of insulin on lipid metabolism in adipocytes. Am. J. Physiol. Endocrinol. Metab. **296**, E635-646

36. Rowland, A.F., Fazakerley, D.J. and James, D.E. (2011) Mapping insulin/GLUT4 circuitry. Traffic **12**, 672-681
37. Sano, H., Kane, S., Sano, E., Mîinea, C.P., Asara, J.M., Lane, W.S., Garner, C.W. and Lienhard, G.E. (2003) Insulin-stimulated phosphorylation of a Rab GTPase-activating protein regulates GLUT4 translocation. J. Biol. Chem. **278**, 14559-14602
38. Berwick, D.C., Hers, I., Heesom, K.J., Moule, S.K. and Tavaré, J.M. (2002) The identification of ATP-citrate lyase as a protein kinase B (Akt) substrate in primary adipocytes. J. Biol. Chem. **277**, 33895-33900
39. Denton, R.M. and Pogson, C.I. (1976) in "Metabolic Regulation", Chapman and Hall, London UK, pp. 49-56
40. Pateel, M.S. and Korotchkina, L.G. (2006) Regulation of the pyruvate dehydrogenase complex. Biochem. Soc. Trans. **34**, 217-222
41. Saggerson, E.D., Sooranna, S.R., Bates, E.J. and Cheng, C.H. (1979) Rapid effects of hormones on enzymes of lipid metabolism. Biochem. Soc. Trans. **7**, 854-857
42. Scott, J.W., Ling, N., Issa, S.M.A., Dite, T.A., O'Brien, M.T., Chen, Z.-P., Galic, S., Langendorf, C.G., Steinberg, G.R., Kemp, B.E. and Oakhill, J.S. (2014) Small molecule drug A-769662 and AMP synergistically activate naïve AMPK independent of upstream kinase signaling. Chem. Biol. **22**, 619-627
43. Ford, R.J., Fullerton, M.D., Pinkosky, S.L., Day, E.A., Scott, J.W., Oakhill, J.S., Bujak, A.L., Smith, B.K., Crane, J.D., Blümer, R.M., Marcinko, K., Kemp, B.E., Gerstein, H.C. and Steinberg, G.R. (2015) Metformin and salicylate synergistically activate liver AMPK, inhibit lipogenesis and improve insulin sensitivity. Biochem. J. **468**, 125-132
44. Holm C. (2003) Molecular mechanisms regulating hormone-sensitive lipase and lipolysis. Biochem. Soc. Trans. **31**, 1120-1124
45. Johanns, M., Lai, Y.-C., Hsu, M.-F., Jacobs, R., Vertommen, D., Van Sande, J., Dumont, J.E., Woods, A., Carling, D., Hue, L., Viollet, B., Foretz, M., Rider, M.H. (2016) AMPK antagonizes hepatic glucagon-stimulated cyclic AMP signalling via phosphorylation-induced activation of cyclic nucleotide phosphodiesterase 4B. Nat. Commun. **7**, 10856
46. Pagnon, J., Matzaris, M., Stark, R., Meex, R.C.R., Macaulay, S.L., Brown, W., O'Brien, P.E., Tiganis, T. & Watt, M.J. (2012) Identification and functional characterization of protein kinase A phosphorylation sites in the major lipolytic protein, adipose triglyceride lipase. Endocrinology **153**, 4278-4289
47. Hoffman, N.J., Parker, B.L., Chaudhuri, R., Fischer-Wellman, K.H., Kleinert, M., Humphrey, S.J., Yang, P., Holliday, M., Trefely, S., Fazakerley, D.J, Stöckli, J., Burchfield, J.G., Jensen, T.J., Jothi, R., Kiens, B., Wojtaszewski, J.F.P., Richter, E.A. and James, D.E. (2015) Global phosphoproteomic analysis of human skeletal muscle reveals a network of exercise regulated kinases and AMPK substrates. Cell Metab. **22**, 922-935
48. Hardie, D.G. (2017) Targeting an energy sensor to treat diabetes. Science **357**, 455-456
49. Longo, M., Zatterale, F., Naderi, J., Parillo, L., Formisano, P., Raciti, G.A., Beguinot, F. and Miele, C. (2019) Adipose tissue dysfunction as determinant of obesity-associated metabolic complications. Int. J. Mol. Sci. **13**, 2358
50. Eissing, L., Scherer, T., Tödter, K., Knippschild, U., Greve, J.W., Buurman, W.A., Pinnschmidt, H.O., Rensen, S.S., Wolf, A.M., Bartelt, A., Heeren, J., Buettner, C. and Scheja, L. (2013) *De novo* lipogenesis of human fat and liver

is linked to ChREBP-β and metabolic health. Nat. Commun. **4**, 1528

Figure legends

Figure 1. Effects of AMPK activators on AMPK activity and AMPKα, ACC and Raptor phosphorylation in rat adipocytes. Adipocytes were incubated with small-molecule AMPK activators at the indicated concentrations or with 0.1% (v/v) DMSO (vehicle control). After 30 min, the cells were harvested and freeze-stopped for homogenization in "Hepes sucrose buffer". Adipocyte extracts were immunoprecipitated with anti-AMPKα1 + anti-AMPKα2 antibodies for AMPK assay (A) or subjected to SDS-PAGE for immunoblotting with anti-phospho Thr172 AMPKα versus anti-total AMPKα (B), anti-phospho Ser79 ACC versus anti-total ACC (C) or anti-phospho Ser792 Raptor versus anti-total Raptor (D) antibodies. Blots were quantified by chemiluminescence and scanning densitometry to calculate relative band intensities obtained with the anti-phospho versus anti-total protein antibodies and representative blots are shown in the upper panels. The values are means ± S.E.M., n = 6 separate experiments (A), n = 3 separate experiments (B), n = 4 separate experiments (C) or n = 5 separate experiments (D). * Indicates a significant effect of AMPK activators versus the DMSO vehicle controls ($P < 0.05$, paired Student's *t*-test).

Figure 2. Dose-dependent AMPK activation by SC4 with and without 0.1 mM AICA riboside in incubated rat adipocytes. Adipocytes were incubated with the indicated concentrations of SC4 with or without 0.1 mM AICA riboside as described in the legend to Figure 1. Adipocyte extracts were immunoprecipitated with anti-AMPKα1 + anti-AMPKα2 antibodies for AMPK assay (A) or subjected to SDS-PAGE for immunoblotting with anti-phospho Thr172 AMPKα versus anti-total AMPK (B) or with anti-phospho Ser79 ACC versus anti-total ACC (C) antibodies. Blots were quantified as described in the legend to Figure 1 and a representative blot is shown in (D). The values are means ± S.E.M., n = 7 separate experiments (A) or n = 4 separate experiments (B, C). * indicates a significant effect of SC4 versus the DMSO vehicle controls ($P < 0.05$, paired Student's *t*-test); † indicates a significant effect of AICA riboside versus SC4 ($P < 0.05$, paired Student's *t*-test).

Figure 3. Effects of SC4 + AICA riboside on noradrenaline-stimulated lipolysis and lipolytic enzyme phosphorylation in incubated rat adipocytes. Adipocytes were preincubated with or without SC4 + AICA riboside for 15 min followed by incubation with the indicated concentrations of noradrenaline as described in the Methods section. After 30 min, the cells were harvested by centrifugation and the incubation media were removed for glycerol assay (A). In (B) freeze-stopped adipocytes were homogenized to obtain fat cake extracts (see Methods section) for SDS-PAGE and immunoblotting with the indicated antibodies (a representative blot is shown in panel C). Blot quantification of relative band intensities obtained with the anti-phospho versus anti-total protein antibodies (see legend to Figure 1) is shown for pSer563 HSL (C), pSer660 HSL (D), pSer565 HSL (E) and pSer406 ATGL (F). The values are means ± S.E.M., n = at least 3 separate experiments. * indicates a significant effect of noradrenaline versus the control incubation without noradrenaline; † indicates a significant effect of SC4 + AICA riboside versus the control incubation

without noradrenaline (F) or versus the incubations with increasing concentrations of noradrenaline alone (A,C,F) ($P < 0.05$, paired Student's *t*-test).

Figure 4. Effects of SC4 + AICA riboside on insulin-stimulated lipogenesis from glucose or acetate in incubated fat pads from WT and AMPKα1 KO mice. The vertical dashed lines indicate that epididymal fat pads from the same animal were incubated pairwise. Fat pads from WT and AMPKα1 KO mice were preincubated with 5 mM glucose or 5 mM glucose + 5 mM acetate with or without SC4 + AICA riboside for 15 min prior to incubation for 60 min with or without insulin in the presence of [^{14}C] glucose (A) or [^{14}C] acetate (B) for measurements of rates of lipogenesis as described in the Methods section. The values are means ± S.E.M., n = 4 (A) or n = 5 (B) separate experiments. In separate experiments, fat pads from WT and AMPKα1 KO mice were incubated with 5 mM glucose but without radioactivity with or without SC4 + AICA riboside with or without insulin as described above for the preparation of extracts, SDS-PAGE and immunoblotting with the indicated antibodies (C-E). Representative blots from n = 5 (C), n = 5 (D) or n = 4 (E) separate experiments are shown. * Indicates a significant effect of insulin versus the controls (white bars); † indicates a significant effect of SC4 + AICA riboside versus insulin alone ($P < 0.05$, paired Student's *t*-test).

Figure 5. Effects of AMPKα1 KO on AMPKα1 and AMPKα2 protein content and AMPKα1 and AMPKα2 activities in mouse fat pads
Fat pads from WT and AMPKα1 KO mice were incubated with 5 mM glucose with or without SC4 + AICA riboside with or without insulin as described in the legend to Figure 4 (C-E) and extracts were immunoblotted for AMPKα1 (A) and AMPKα2 (B) for quantification versus GAPDH as described in the legend to Figure 1 or immunoprecipitated for measurements of AMPKα1 (C) and AMPKα2 activity (D). The results are means ± S.E.M., n = 12 separate determinations (A,B) or means ± S.E.M., n = 5 (C) or n = 3 (D) separate determinations. * Indicates a significant effect of AMPKα1 KO versus the WT controls (white bars); † indicates a significant effect of SC4 + AICA riboside versus insulin alone ($P < 0.05$, paired Student's *t*-test).

Figure 6. Effects of SC4 + AICA riboside on insulin-stimulated lipogenesis and ACC phosphorylation in incubated fat pads from WT versus ACC1/2 S79A/S212A KI mice. Fat pads from WT versus ACC1/2 S79A/S212A KI mice were incubated as described in the legend to Figure 4 to measure rates of lipogenesis from [^{14}C] acetate (A). In separate experiments, fat pads from S79A/S212A KI mice were incubated with 5 mM glucose with or without SC4 + AICA riboside with or without insulin as described in the legend to Figure 4 for the preparation of extracts, SDS-PAGE and immunoblotting with the indicated antibodies (B). Blots were quantified as described in the legend to Figure 1 and a representative blot is shown in the upper panel. The values are means ± S.E.M., n = 7 (A) or n = 3 (B) separate experiments. * Indicates a significant effect of insulin versus the controls (white bars); † indicates a significant effect of SC4 + AICA riboside versus insulin alone ($P < 0.05$, paired Student's *t*-test). ¶ Indicates a significant effect of ACC1/2 double KI versus the WT ($P < 0.05$, unpaired Student's *t*-test).

Figure 7. Effects of of SC4 + AICA riboside on insulin-stimulated glucose uptake in incubated fat pads from WT versus AMPKα1 KO mice. The vertical dashed lines indicate that epididymal fat pads from the same animal were incubated

pairwise. Fat pads from WT (A) or WT versus AMPKα1 KO mice (B) were preincubated with [^{14}C] 2-deoxyglucose and non-radioactive 2-deoxyglucose with and without SC4 + AICA riboside for 15 min followed by incubation for 60 min with or without insulin. The values are means ± S.E.M., n = 5 (A) or n = 4 (B) separate experiments. * Indicates a significant effect of insulin versus the vehicle controls; † indicates a significant effect of SC4 + AICA riboside versus insulin alone (P < 0.05, paired Student's t-test).

Figure 8. Effects of SC4 + AICA riboside and insulin on PKB, AMPKα, ACC, TBC1D4 and ACL phosphorylation in incubated mouse fat pads. The vertical dashed lines indicate that epididymal fat pads from the same animal were incubated pairwise. Fat pads from WT mice were preincubated with SC4 + AICA riboside and 5 mM glucose for 15 min followed by incubation with or without insulin for 60 min. The fat pad pieces were harvested by flotation, freeze-stopped and homogenized in "Hepes sucrose buffer". Following centrifugation, extracts were subjected to SDS-PAGE for immunoblotting with anti-phospho Ser473 PKB and anti-total PKB antibodies (A), anti-phospho Thr308 PKB and anti-total PKB antibodies (B), anti-phospho Thr172 AMPKα and anti-total AMPKα antibodies (C), anti-phospho Ser79 ACC and anti-total ACC antibodies (D), anti-phospho Thr642 TBC1D4 and anti-total TBC1D4 antibodies (E) and anti-phospho Ser454 ACL and anti-total ACL antibodies (F). Blots were quantified as described in the legend to Figure 1 and representative blots are shown in the upper panels. The values are means ± S.E.M., for n = 4 (A), n = 3 (B), n = 4 (C), n = 3 (D), and n= 5 (E, F) separate experiments. * Indicates a significant effect of insulin versus the vehicle controls; † indicates a significant effect of SC4 + AICA riboside versus insulin alone (P < 0.05, paired Student's t-test).

Figure 9. Effects of SC4 + AICA riboside on insulin-stimulated esterification and GPAT activity in incubated mouse fat pads.
The vertical dashed lines indicate that epididymal fat pads from the same animal were incubated pairwise. Fat pads from WT mice were preincubated with SC4 + AICA riboside and 5 mM glucose + 0.5 mM palmitate for 15 min prior to incubation for 60 min with or without insulin in the presence of [^{3}H] palmitate for measurements of rates of esterification as described in the Methods section (A). Fat pads extracts from the experiment shown in Figure 7 were assayed for total GPAT activity (B). The values are means ± S.E.M., n = 3 separate experiments. * Indicates a significant effect of insulin versus the vehicle controls (P < 0.05, paired Student's t-test).

Fig. 1

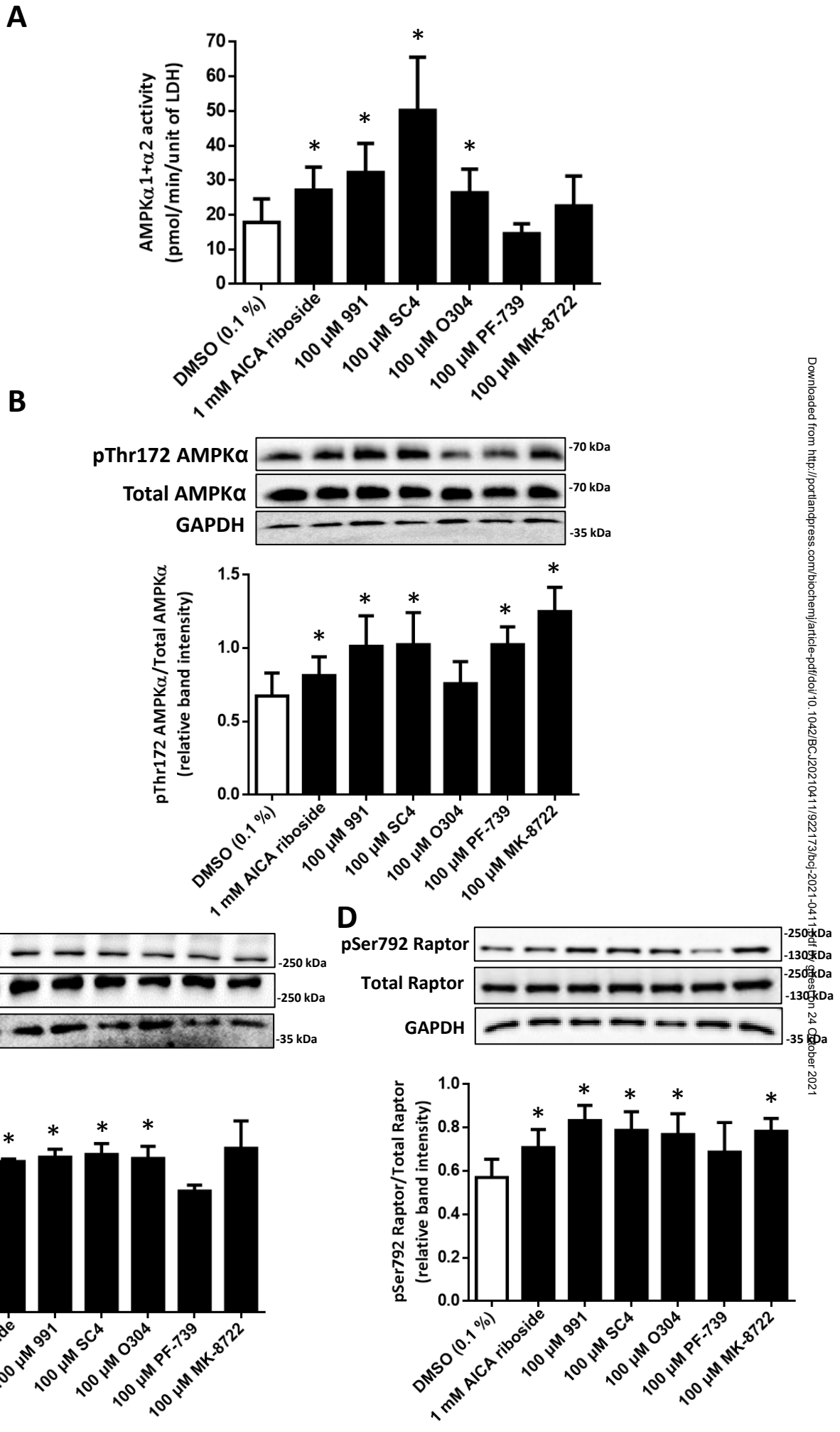

Fig. 2

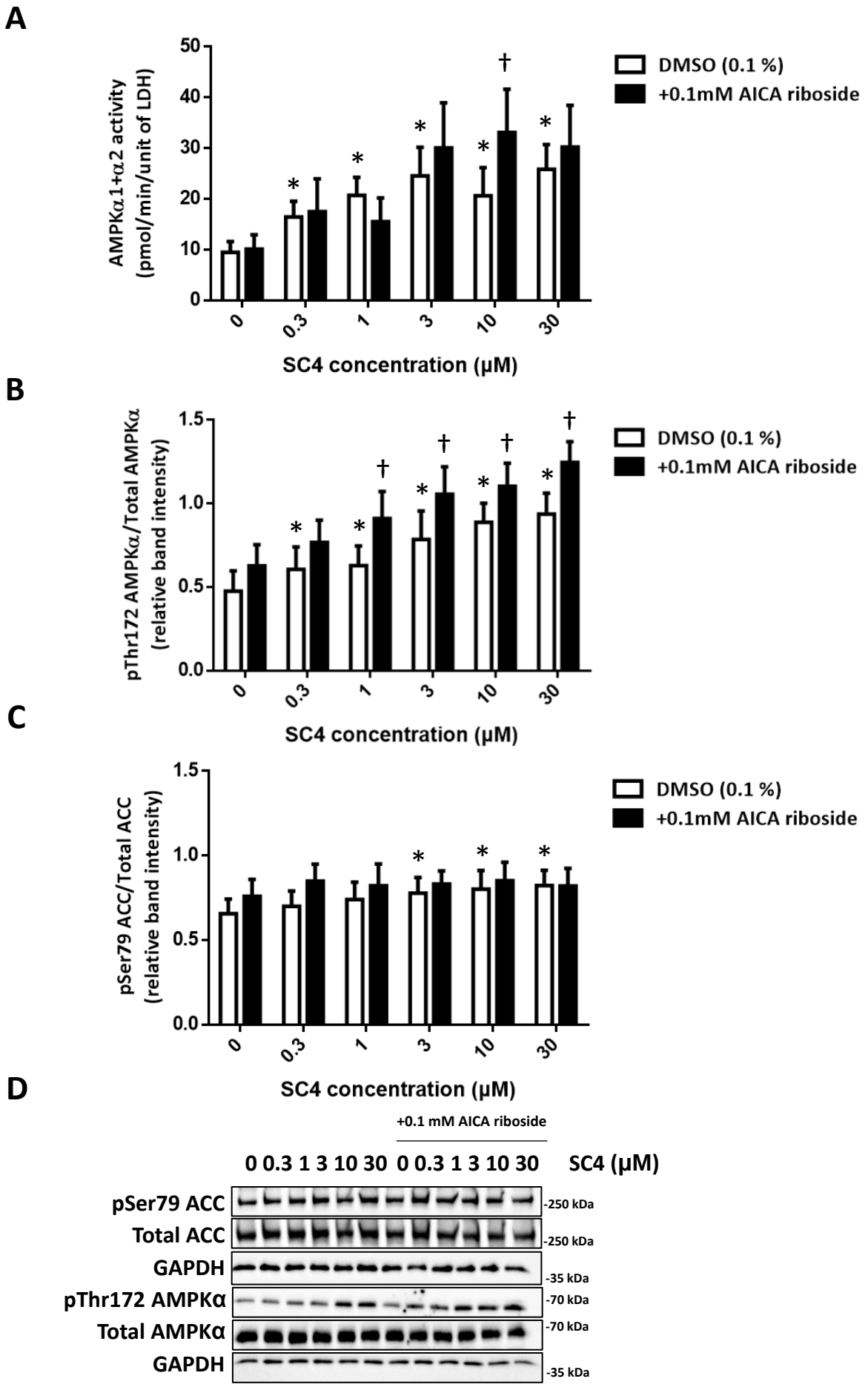

Fig. 3

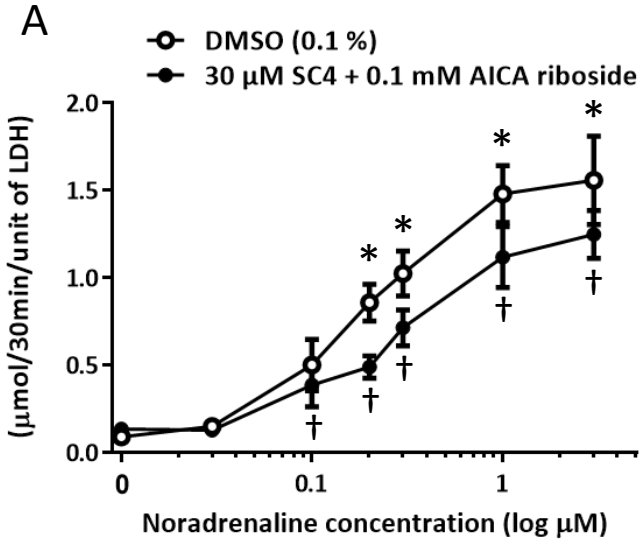

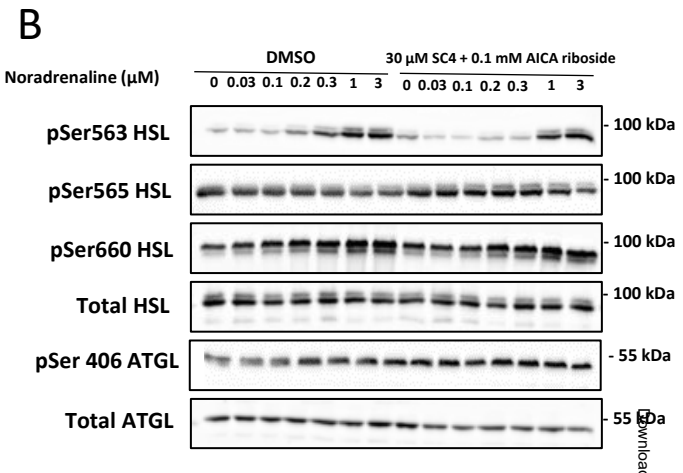

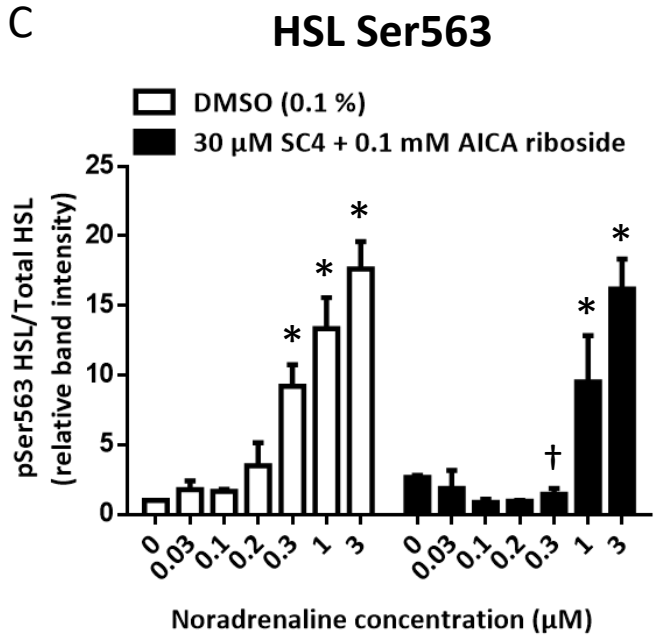

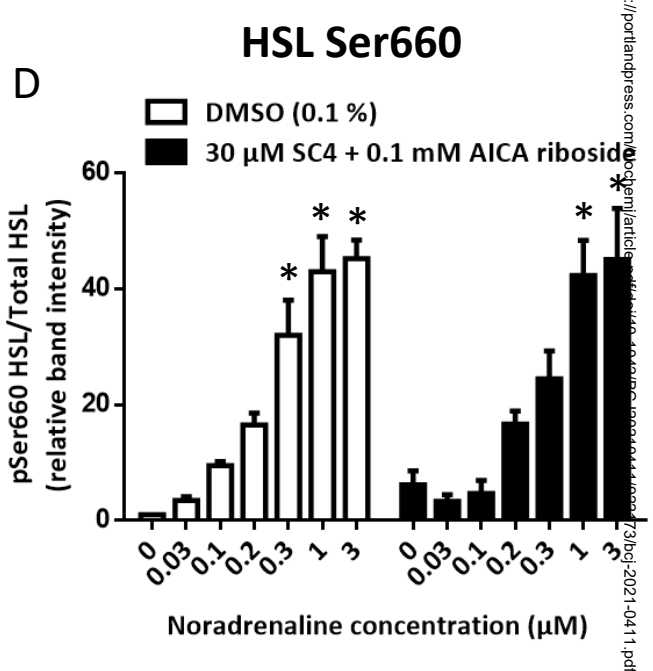

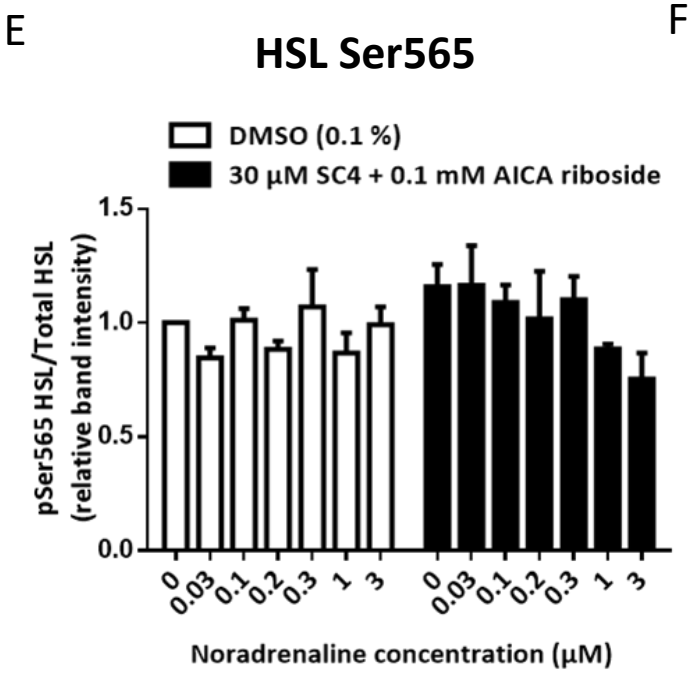

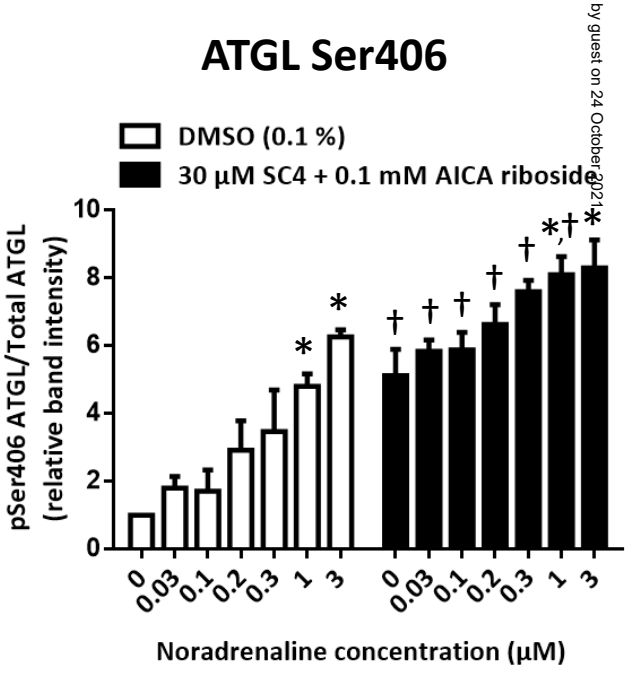

Fig. 4

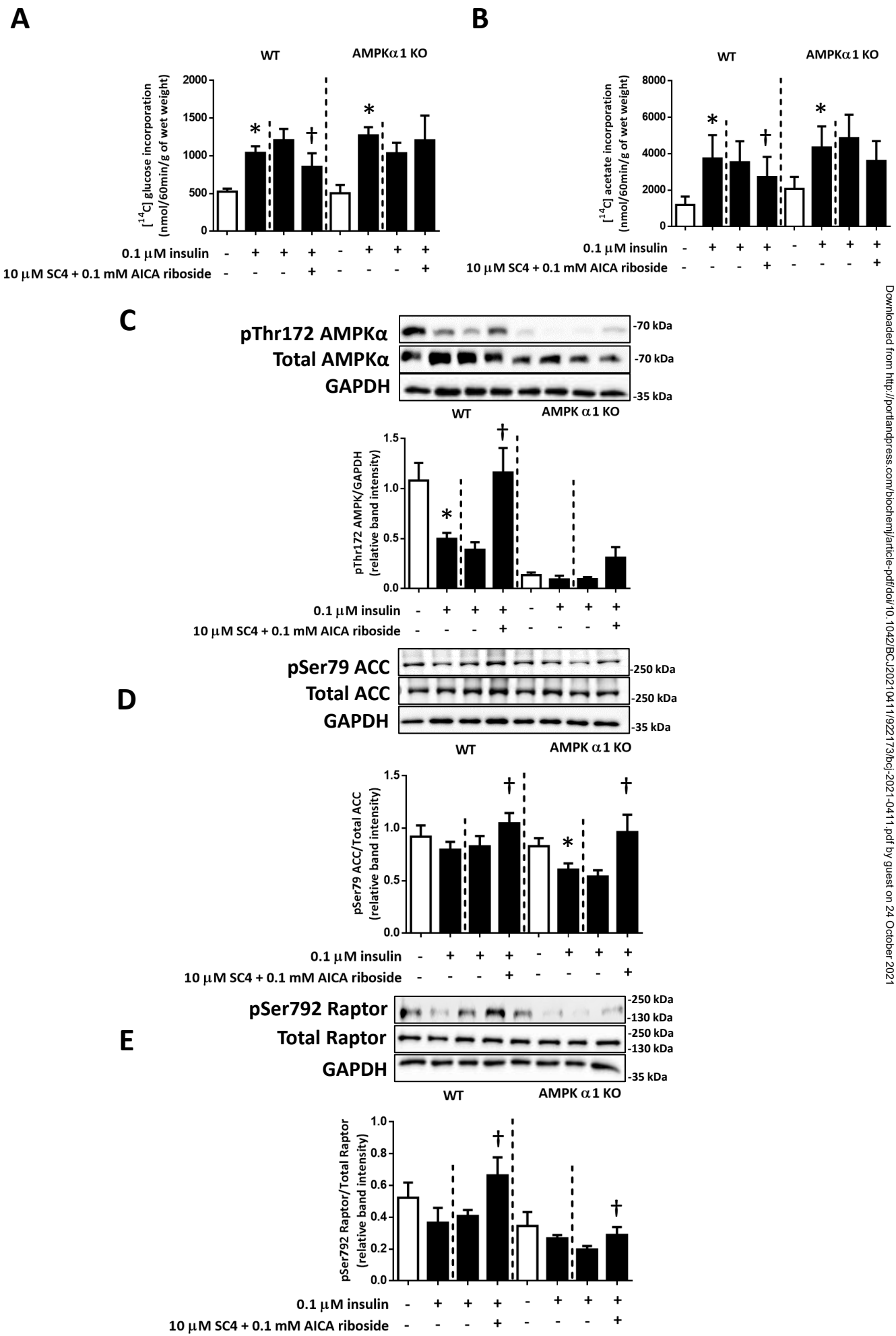

Fig. 5

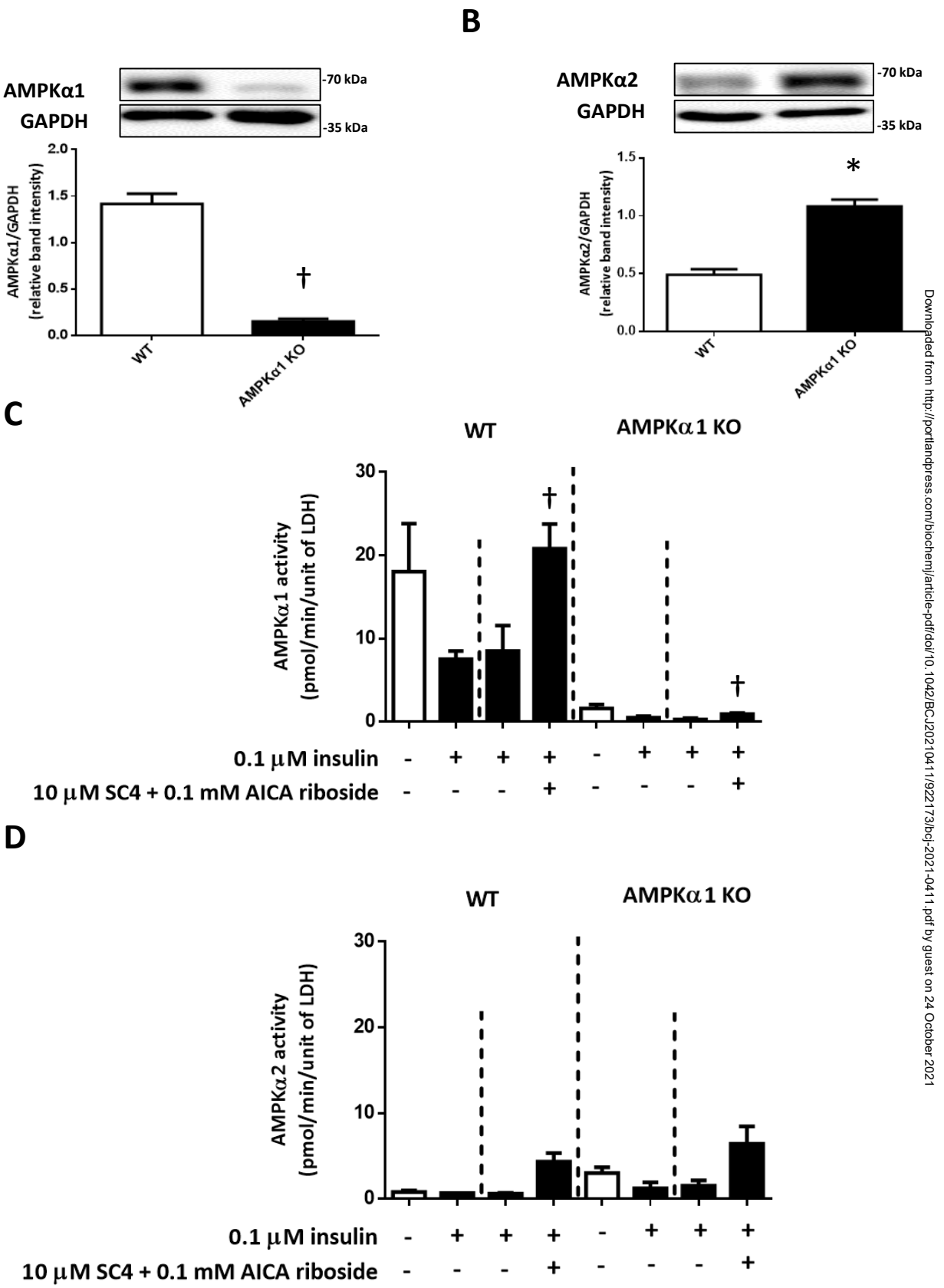

Fig. 6

A

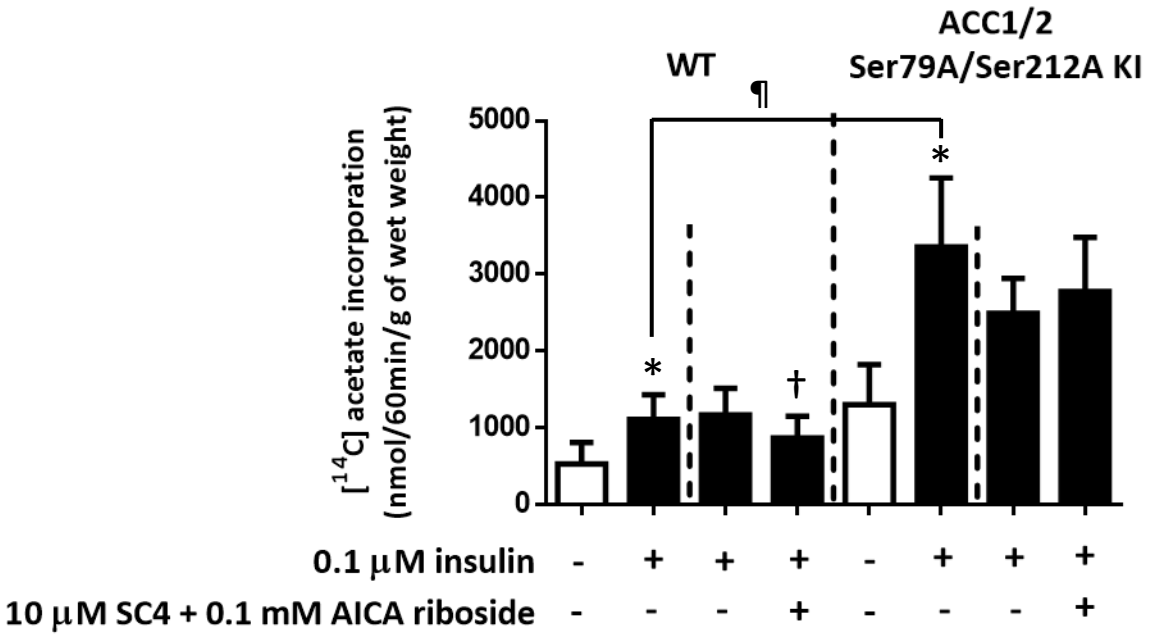

B

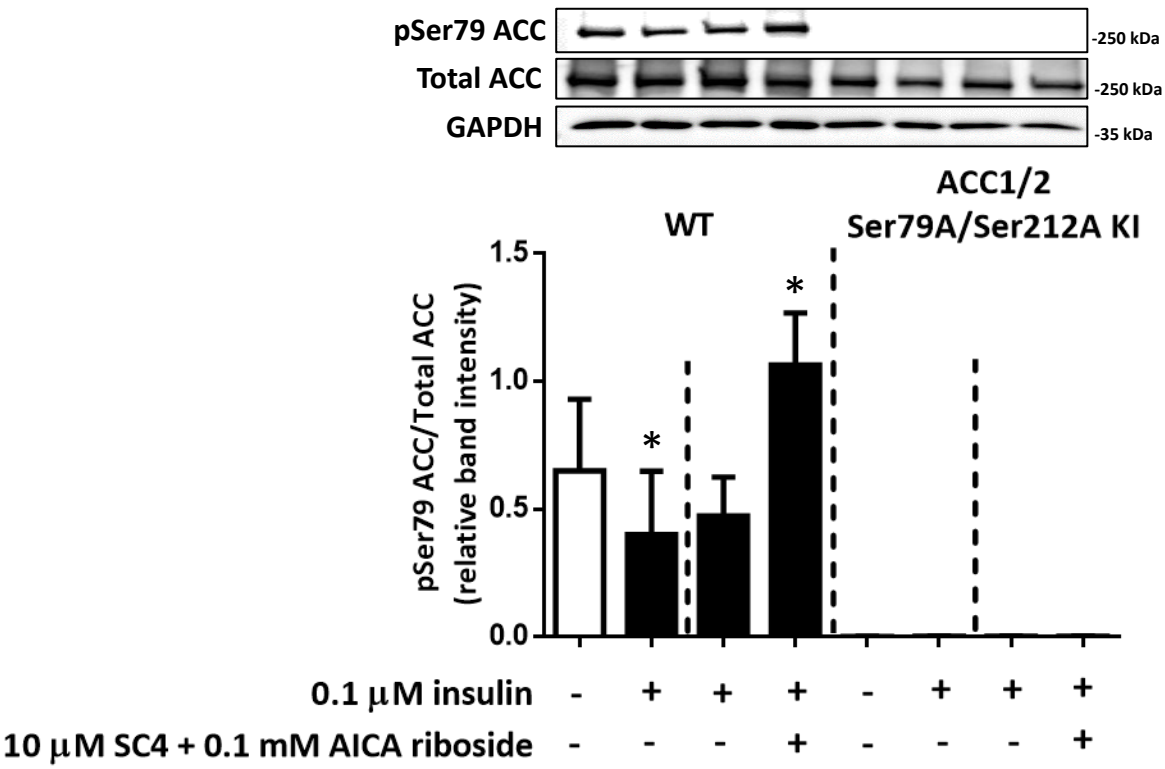

Fig. 7

A

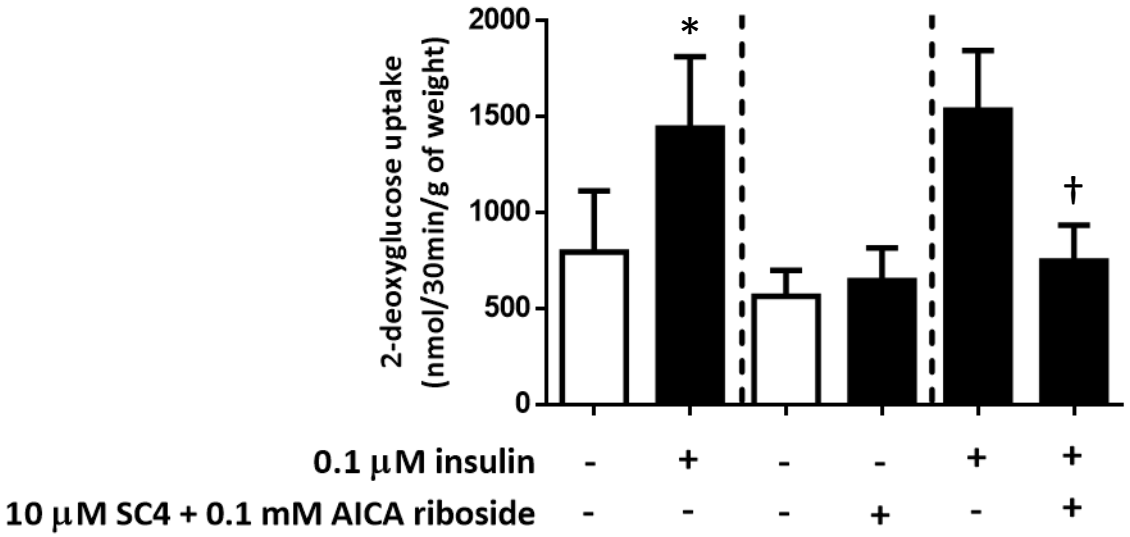

B

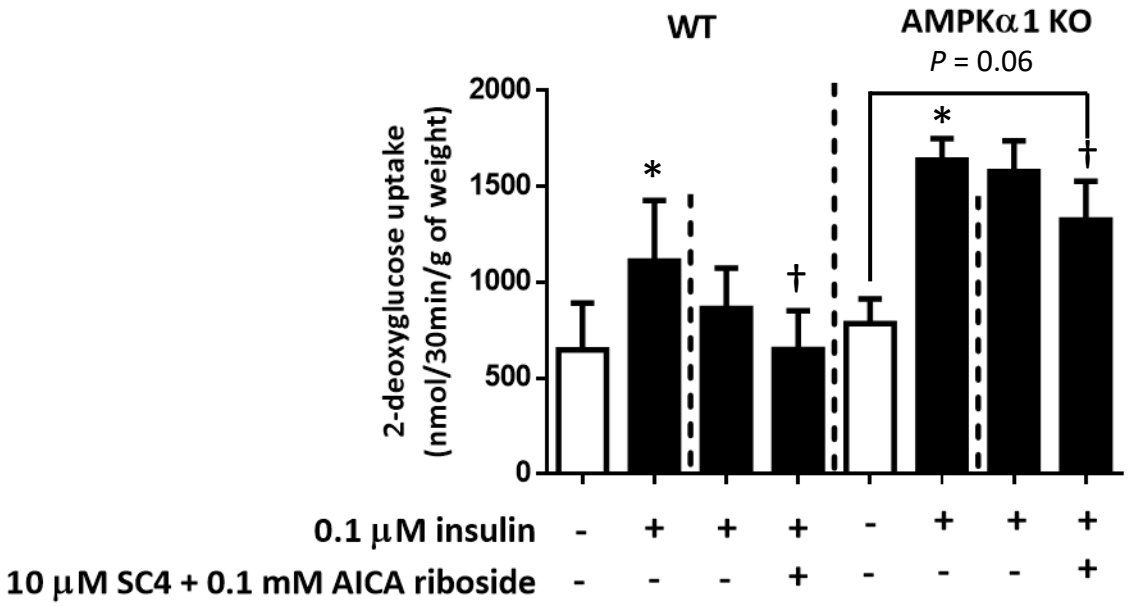

Fig. 8

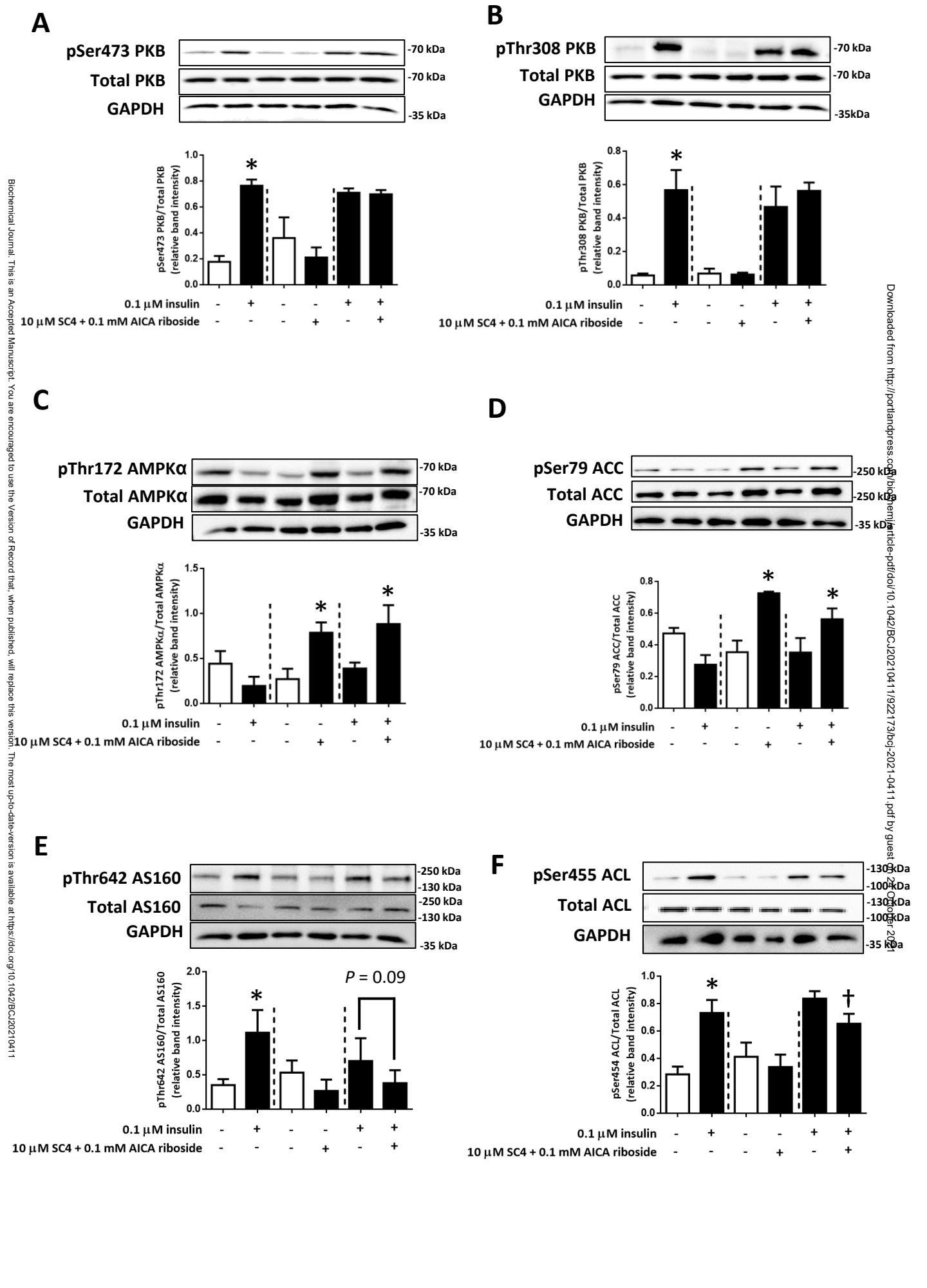

Fig. 9

A

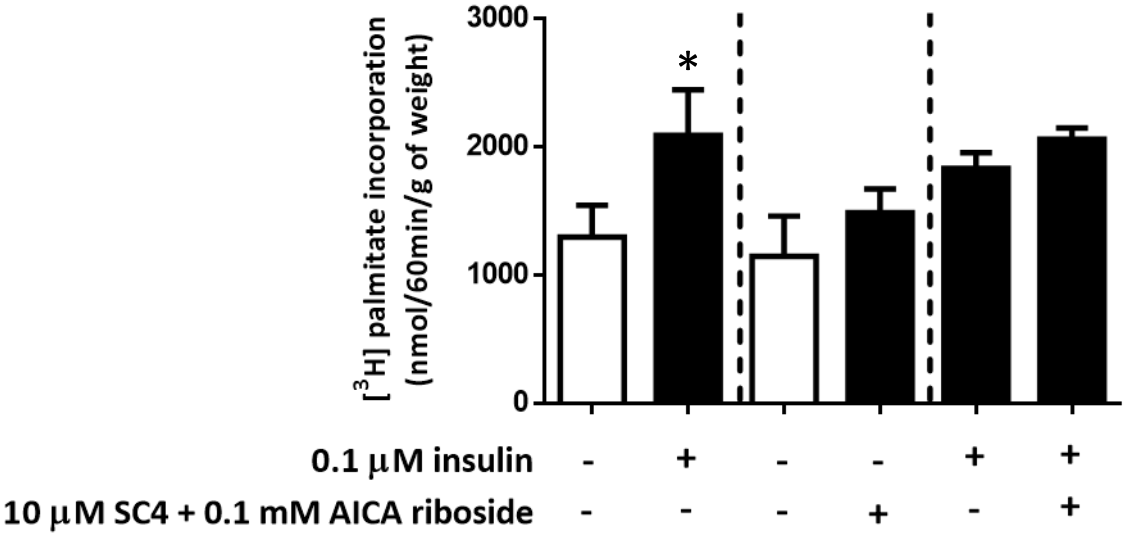

B